12-2018

Sea-Level Rise in the Humboldt Bay Region - Update 2

Jeffrey K. Anderson

Sea-Level Rise in the Humboldt Bay Region

Update 2: December 2018

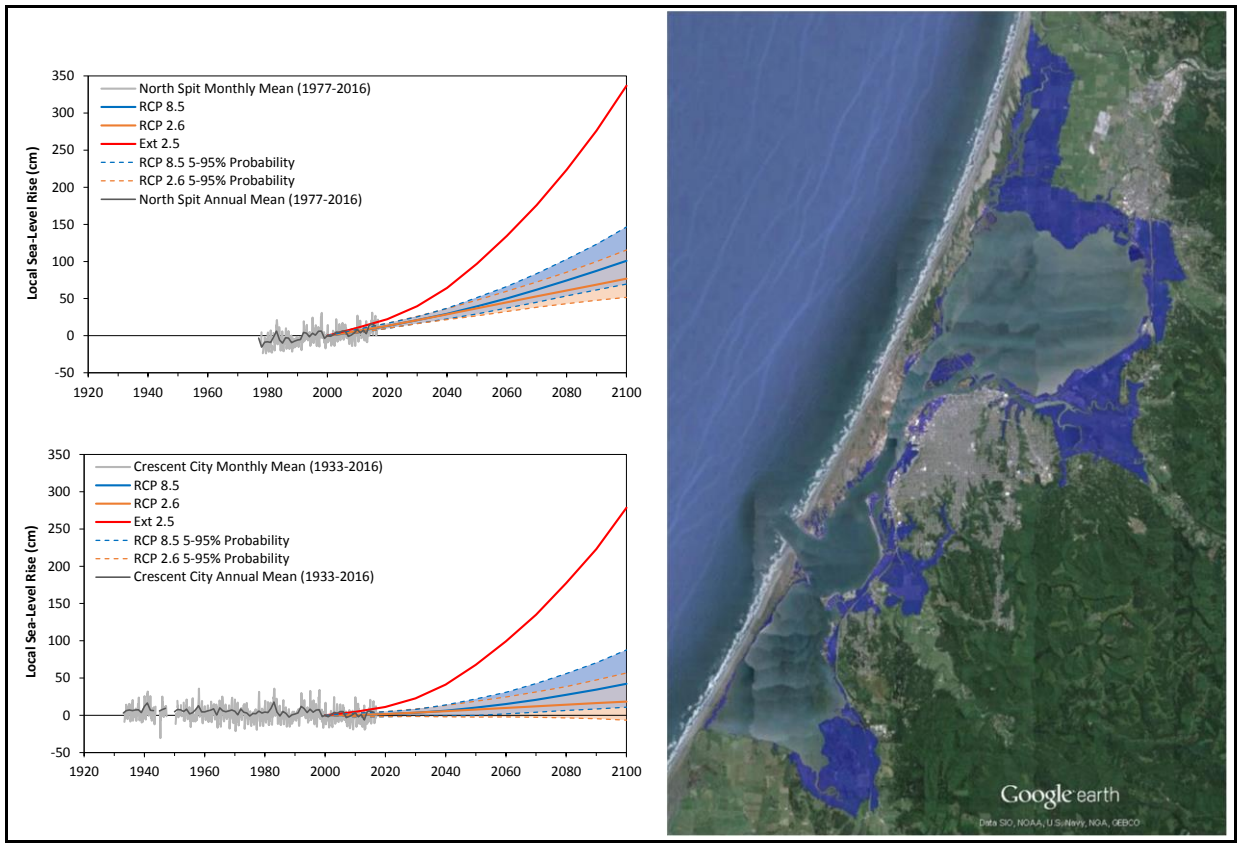

Prepared by

Jeffrey K. Anderson
Northern Hydrology & Engineering
P.O. Box 2515
McKinleyville, CA 95519

Northern Hydrology & Engineering

Preparation of this document was partially funded by the City of Arcata.

Sea-Level Rise in the Humboldt Bay Region

Sea-level rise is one of the most evident and problematic consequences of global climate change. As the earth's climate warms, sea levels increase primarily from thermal expansion of a warmer ocean and melting land ice (NRC, 2012). In California, sea-level rise will threaten and directly affect vulnerable coastal ecosystems, bays and estuaries, coastal communities and infrastructure due to increased flooding, gradual inundation, and erosion of the coastal shorelines, cliffs, bluffs and dunes (Russell and Griggs, 2012). If sea level continues to rise at present rates, identified impacts could take decades or longer to occur. However, a troublesome aspect of climate change and the rapid warming of the earth's atmosphere and ocean is the potential for sea-level rise to accelerate to high rates over a short period of time, in which case the identified impacts could happen within a much shorter period (years to decades). Although there is uncertainty in the timing of sea-level rise and future impacts, society still needs to plan for, and adapt to higher sea levels.

The coasts of Humboldt and Del Norte Counties are experiencing the combined effects of global sea-level rise, regional sea-level height variability from seasonal to multidecadal ocean-atmosphere circulation dynamics (e.g. El Niño Southern Oscillation (ENSO)), and relatively large tectonic vertical land motions associated with the Cascadia subduction zone (CSZ) (Figure 1). These large tectonic motions along the southern CSZ create the highly variable and opposing sea-level trends observed between Humboldt Bay and Crescent City. Recent estimates of land subsidence by Patton et al. (2017) indicate that Humboldt Bay has the highest local sea-level rise rate in California, approximately two to three times higher than the long-term global rate. In contrast, the land in Crescent City (109 km north) is uplifting faster than long-term global sea level rise, which causes a negative or decreasing local sea-level rise rate.

Overview and Purpose

The purpose of this chapter is to provide an overview of global and regional sea-level rise, with an emphasis on physical processes locally affecting sea levels in the Humboldt Bay region and provides an update to Chapter 2 of the Humboldt Bay: Sea Level Rise, Hydrodynamic Modeling, and Inundation Vulnerability Mapping report (NHE, 2015a). This overview relies on the past climate and sea-level change literature (e.g. NRC, 2012; IPCC, 2013; Church et al., 2013), the more recent sea-level science literature (e.g. Kopp et al., 2014; Kopp et al., 2015; Hall et al., 2016; Sweet et al., 2017; Griggs et al., 2017), the scientific and technical literature specific to the U.S. Pacific Northwest (PNW) coast (e.g. Burgette et al., 2009; Komar et al, 2011), and literature specific to the Humboldt Bay region (e.g. NHE, 2015a; Patton et al., 2017).

In 2017, the Ocean Protection Council (OPC) Science Advisory Team released its updated sea-level rise science report, titled Rising Seas in California: An Update on Sea-Level Rise Science (Griggs et al., 2017). The OPC report provides an update on the current state of sea-level rise science, along with a synthesis of the current scientific understanding of potential Greenland and

Antarctic ice sheet loss and implications for sea-level rise projections in California. The OPC report also provided probabilistic sea-level rise projections at three locations along the California coast (Crescent City, San Francisco, and La Jolla) based on the approach of Kopp et al. (2014).

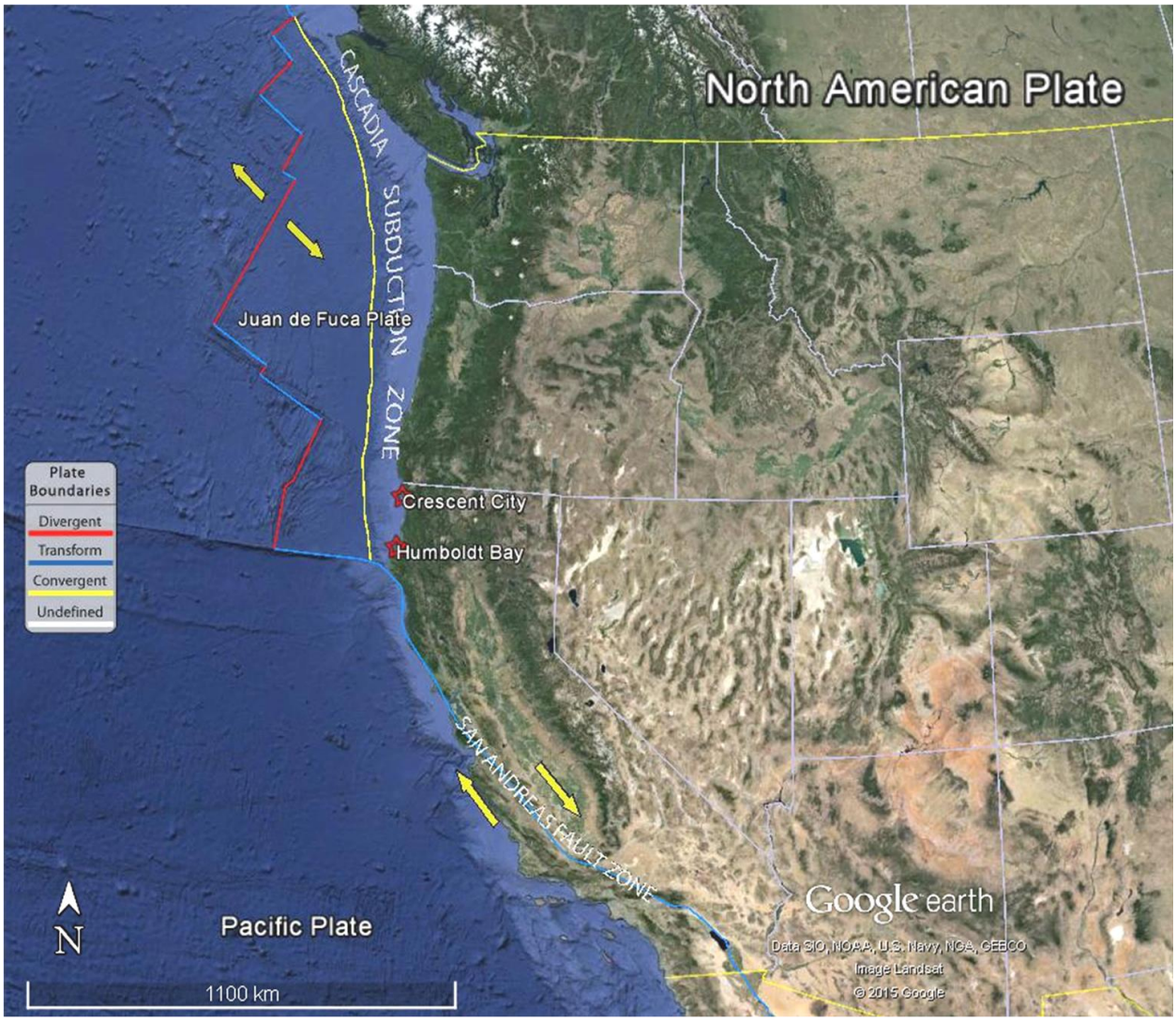

Figure 1. Tectonic plate boundaries along the U.S. west coast, and the location of Humboldt Bay and Crescent City relative to the Cascadia subduction zone. Tectonic boundary data downloaded from http://earthquake.usgs.gov/learn/kml.php.

The OPC (2017) report did not address local issues affecting sea-level rise in the Humboldt Bay region or provide projections applicable for the region. A key purpose of this chapter is to provide probabilistic sea-level rise projections for the Humboldt Bay region based on the work of Kopp et al. (2014) and the local estimates of vertical land motion by Patton et al. (2017). The updated overview and probabilistic projections provide decision makers the most up-to-date and

locally relevant information to support planning and developing adaptation strategies for sea-level rise in the Humboldt Bay region.

Global Climate System Change

In 2013, the IPCC completed its Fifth Assessment Report (AR5). The AR5 states that continued emissions of greenhouse gases (carbon dioxide, methane, and nitrous oxide) will cause changes in all components of the global climate system, affecting temperature and precipitation patterns, ocean temperatures and chemistry, ocean-climate variability, and sea-level rise. The AR5 reports (95% confidence) that human activity is the dominant cause of the observed global climate system warming since the mid-20th century (Figure 2), with the last three decades being successively warmer than any preceding decade since 1850. Furthermore, atmospheric concentrations of greenhouse gases have increased to levels unprecedented in at least the last 800,000 years. Carbon dioxide concentrations have increased by 40% since pre-industrial times, with the ocean absorbing about 30% of the emitted anthropogenic carbon dioxide (Figure 3), causing ocean acidification (IPCC, 2013). The AR5 concluded that limiting climate change will require substantial and sustained reductions of greenhouse gas emissions.

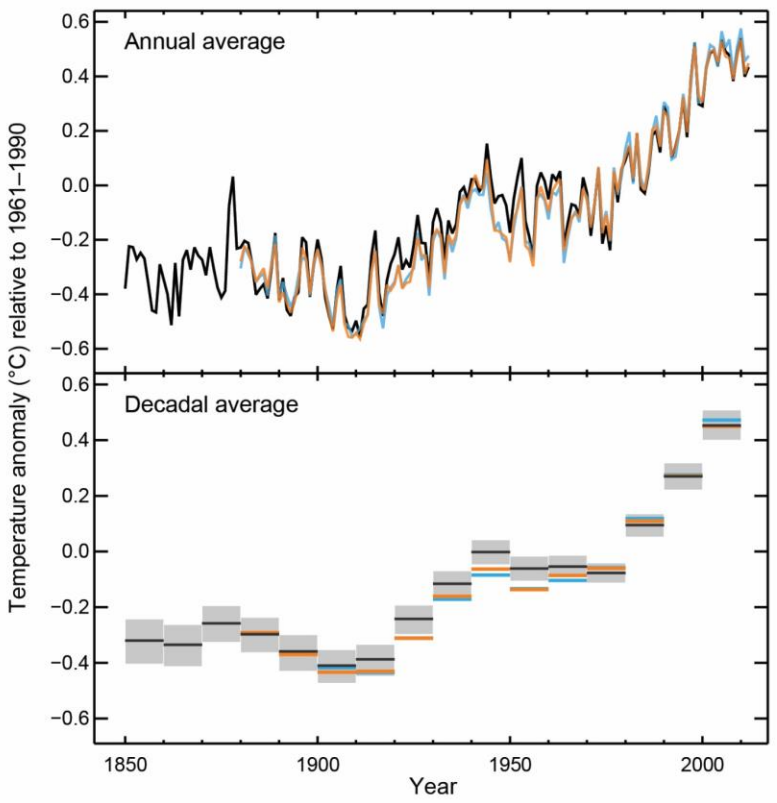

Figure 2. Observed 1850 to 2012 global mean combined land and ocean surface temperature anomalies (relative to the mean of 1961-1990) from three datasets. Top panel is the annual mean values, and bottom panel are the decadal mean values with uncertainty for one dataset (black). (Figure from IPCC, 2013)

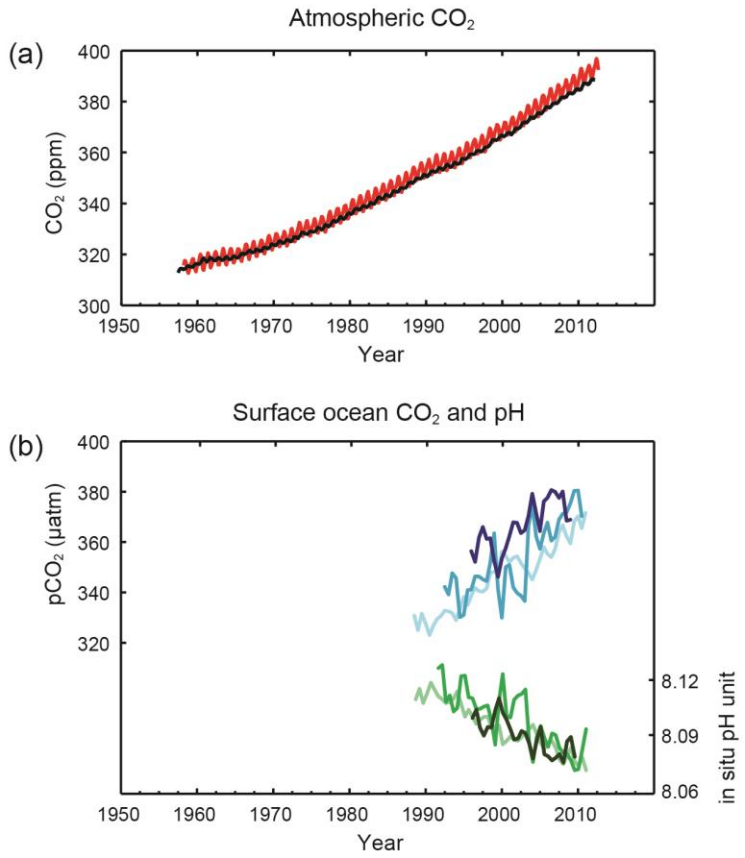

Figure 3. (a) Observed atmospheric carbon dioxide (CO_2) concentrations for Mauna Loa (red line) and South Pole (black line) since 1958. (b) Ocean surface observed partial pressure of dissolved CO_2 (blue lines), and in situ pH (green lines) which is an indicator of ocean acidification. Measurements from Atlantic Ocean (dark blue and dark green, and blue and green) and Pacific Ocean (light blue and light green). (Figure from IPCC, 2013)

Past and Present Sea-Level Rise

This section provides an overview of sea-level change associated with global mean sea-level (GMSL) rise, regional sea-level (ReSL) rise, and local sea-level (LSL) rise.

Global Mean Sea-Level

Global mean sea levels have been increasing since the last ice age about 20,000 years ago (Russell and Griggs, 2012; Kominz, 2001), although at relatively low rates (~ 0.1 mm/yr) over the last two millennia (NRC, 2012). There is high confidence, based on proxy records (e.g. salt marsh sediments) and instrumental sea-level data, that GMSL rise increased in the late 19th to early 20th century from relatively low rates over the previous two millennia to higher rates today (Church et al., 2013). The dominant contributors to GMSL rise over the last century are atmospheric and ocean warming, which increases ocean volume through ocean thermal expansion, and increases ocean mass from melting land ice and, to a lesser extent, land water storage and groundwater extraction (Rhein et al., 2013; Church et al., 2013).

Analysis of global tide gauge records dating back to the 1880s (Church and White, 2011), and the more recent satellite altimetry observations of sea surface change from 1993 to present (Beckley et al., 2010) clearly indicate that GMSL rise rates have increased since 1993 (Figure 4, Table 1). The tide gauge reconstructions by Church and White (2011) indicate that the rate of GMSL rise between 1901 to 1990 was 1.5 ± 0.2 mm/yr, and from 1901 and 2010 was 1.7 ± 0.2 mm/yr. The rate of GMSL rise measured by satellite altimetry from 1993 to 2016 is 3.4 ± 0.4 mm/yr (https://sealevel.nasa.gov, data accessed in September 2017), which is two times or more the tide gauge rates listed above. Recently, Hay et al. (2015) reanalyzed the tide gauge data using probabilistic techniques and estimated a GMSL rise rate of 1.2 ± 0.2 mm/yr from 1901 to 1990, which is lower than the Church and White (2011) estimate for the same period. This indicates that the increase in GMSL rates from 1993 to 2016 (altimetry rate of 3.4 ± 0.4 mm/yr) over the 1901 to 1990 rates is greater than previously thought (Hay et al., 2015). Although these methods result in different estimates of the rate of GMSL rise, they all indicate the same overall pattern of increased rates in recent decades.

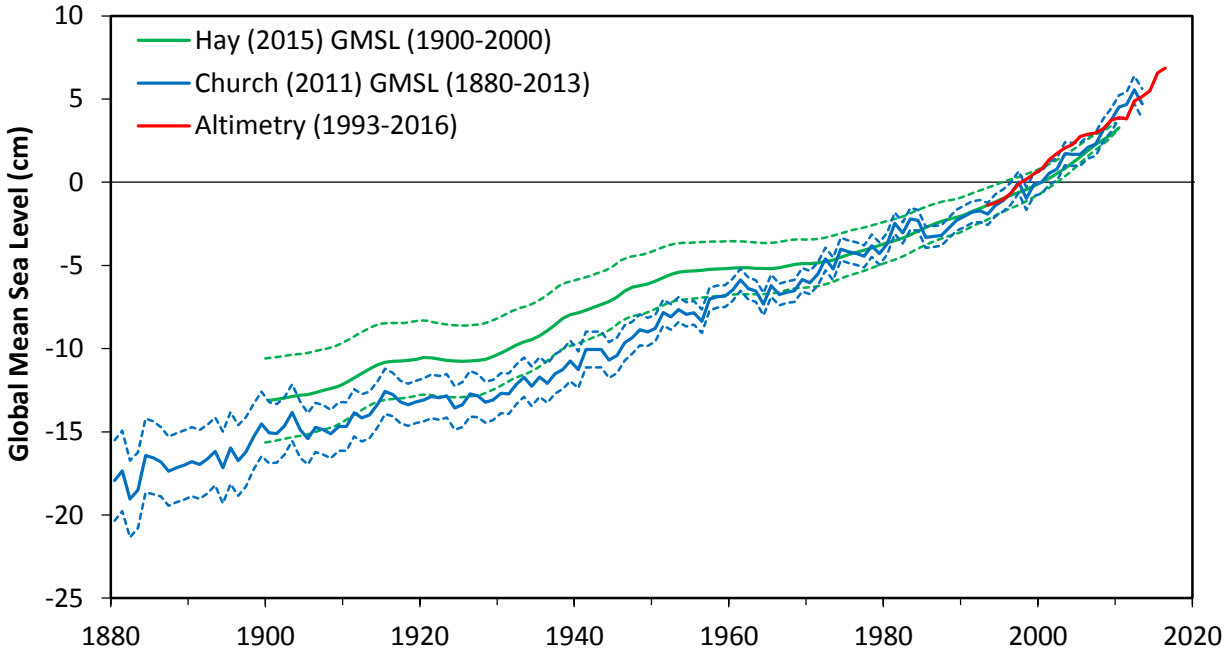

Figure 4. Yearly average reconstructed GMSL (blue line) for 1880 to 2013 of Church and White (2011) with one standard deviation uncertainty bounds (blue dashed line), data downloaded from http://www.cmar.csiro.au. Reconstructed GMSL (green line) for 1901 to 2010 of Hay et al. (2015) with one standard deviation uncertainty bounds (green dashed line), data downloaded with publication. Satellite altimeter data for 1993 to 2016 of Beckley et al. (2010), data downloaded at: https://sealevel.nasa.gov. All data relative to year 2000 baseline.

Table 1. Estimated GMSL rise rates and uncertainty range (90% confidence interval) for different time periods. Data from Church and White (2011), Hay et al. (2015), Rhein et al. (2013) and Beckley et al. (2010).

Time Period	GMSL Rise Rate and Uncertainty (mm/yr)	Source
1901 to 1990	1.5 [1.3 to 1.7]	Tide gauge reconstruction (Church and White, 2011)
1901 to 1990	1.2 [1.0 to 1.4]	Tide gauge reconstruction (Hay et al., 2015)
1901 to 2010	1.7 [1.5 to 1.9]	Tide gauge reconstruction (Church and White, 2011)
1993 to 2016	3.4 [3.0 to 3.8]	Satellite altimetry data (Beckley et al., 2017)

Regional Sea-Level Rise

As mentioned above, the dominant drivers to GMSL rise are thermal expansion of the ocean, increases in ocean mass from melting land ice, and to a lesser extent, changes in land water storage. However, the spatial or ReSL rise can differ from GMSL rise due to a range of factors such as ocean dynamics, climate variability, and sea-level fingerprints (Cayan et al., 2008; NRC, 2012; Church et al.,2013; Kopp et al., 2014; Kopp et al., 2015). Figure 5 shows the monthly mean LSL rise trends at three NOAA long-term (greater than 100-years) tide gauges located on relatively tectonically stable ground (Cayan et al., 2008; Burgette et al., 2009; Bromirski et al., 2011). The three sea-level rise trends are consistent, ranging from 1.94 to 2.15 mm/yr, with the average (2.0 mm/yr) representing an estimate of ReSL rise along the U.S. west coast. This rate is 18% greater than the 1901 to 2010 GMSL trend of 1.7 mm/yr (Table 1), implying that over the instrument period ReSL rise along the U.S. west coast has been greater than GMSL rise. The dominant factors affecting ReSL change along the U.S. west coast are summarized below.

Ocean Dynamics and Climate Variability. Non-uniform sea-level changes arise from ocean dynamics, circulation, heat content, and salinity differences due to freshwater (mass) inputs from ice loss, regional wind and current patterns, and coupled ocean-atmosphere processes from natural climate variability. The most important climate processes along the U.S. west coast affecting sea-level change are the seasonal cycle, ENSO, and the Pacific Decadal Oscillation (PDO) (Komar et al., 2011; Bromirski et al., 2011; NRC, 2012).

Seasonal coastal current and wind patterns (e.g. upwelling) produce variations in sea levels, known as the average seasonal cycle, due to ocean temperature and density changes (Zervas, 2009; Komar et al., 2011). ENSO causes seasonal to interannual timescale climate variability with more active winter storm periods and higher sea levels during the warmer El Niño phase, and lower levels during the cooler La Niña phase (Figure 6). The PDO is described as an interdecadal ENSO like pattern of climate variability in the Pacific Ocean with warm and cool phases (Figure 6) that shift on interdecadal timescales of about 20 to 30 years (Zhang et al., 1997; Mantua et al., 1997).

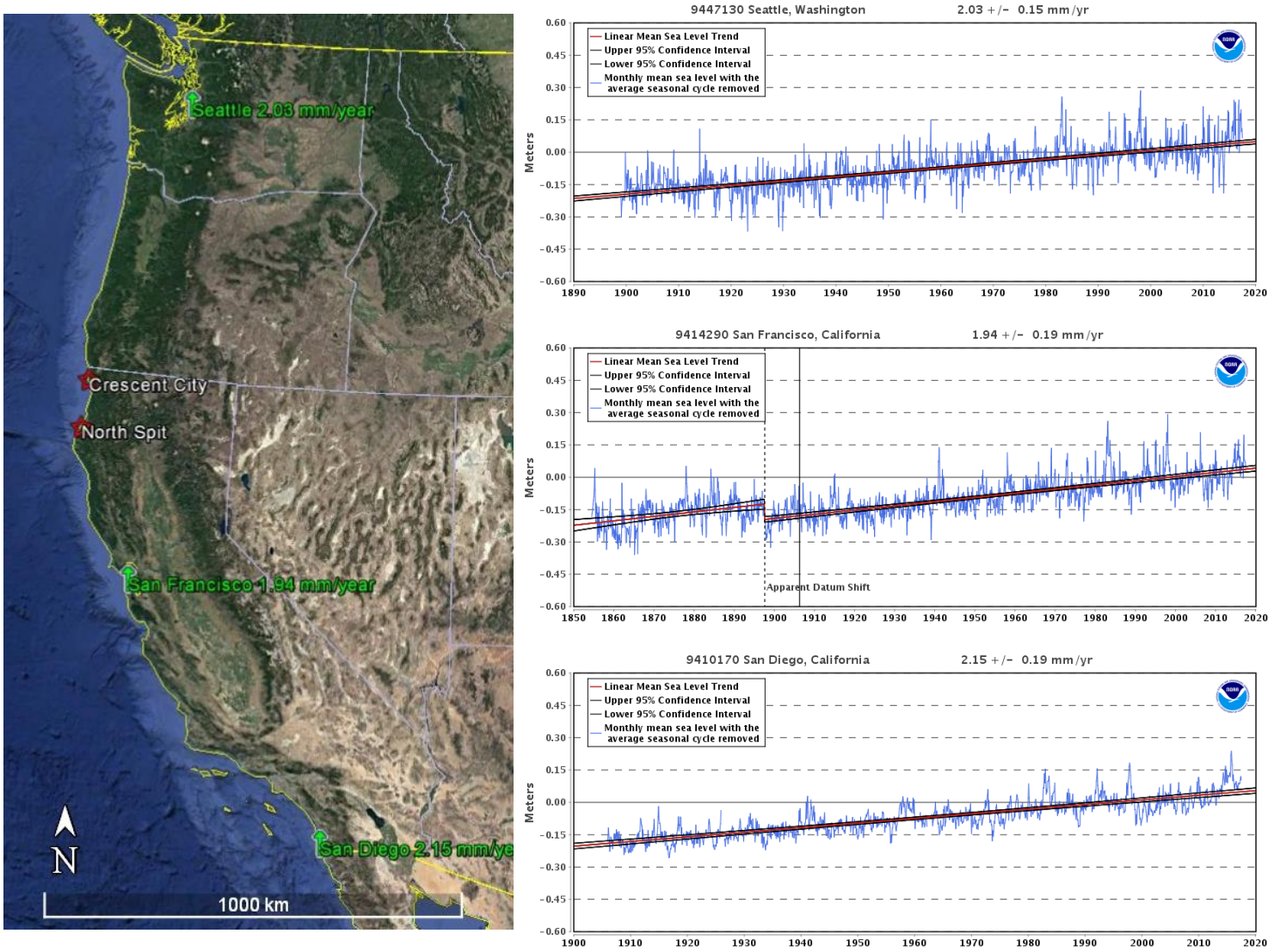

Figure 5. Observed monthly ReSL rise trends for NOAA tide gauge records for Seattle, San Francisco and San Diego. These tide gauge sites are located on relatively tectonically stable ground. Data and figures accessed on October 2017 at http://tidesandcurrents.noaa.gov.

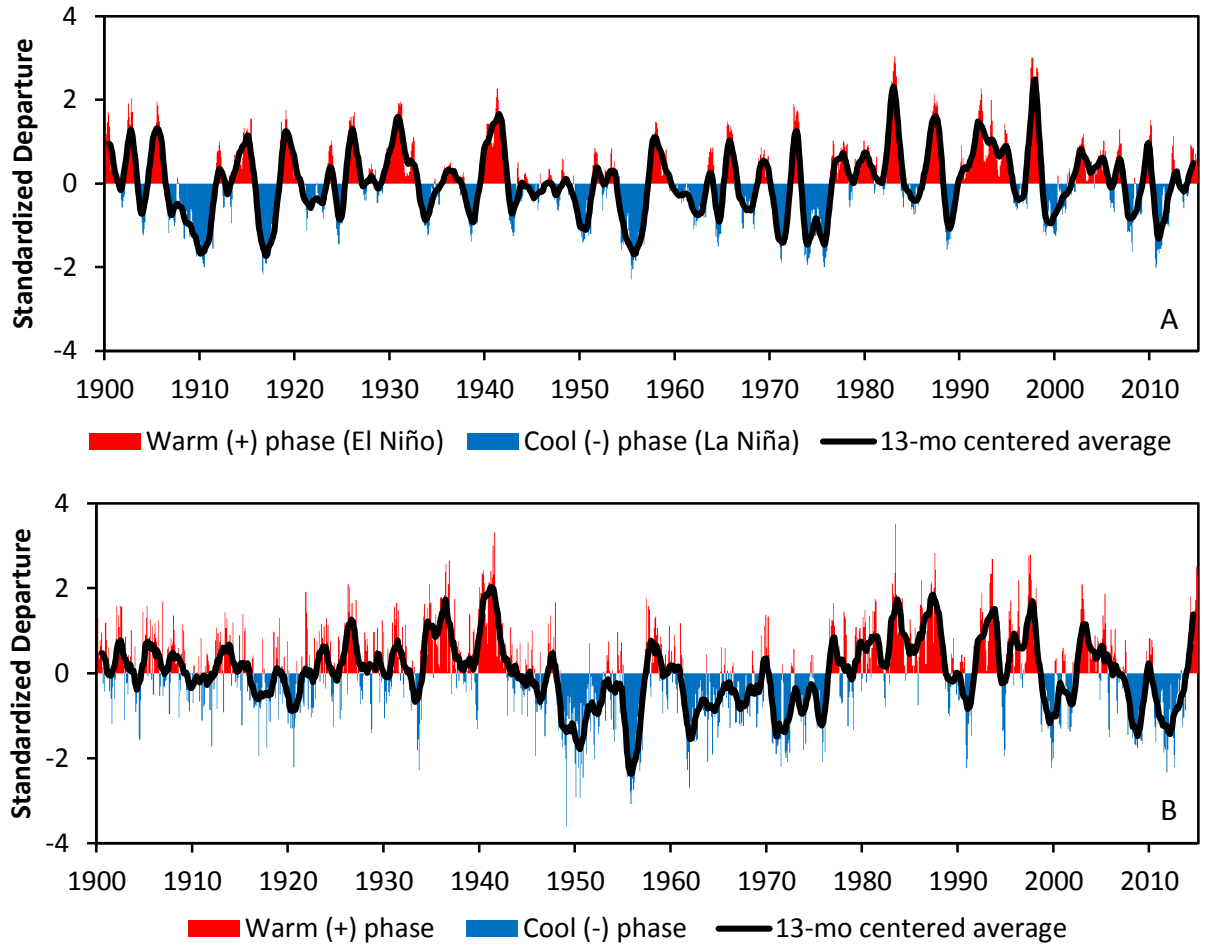

Figure 6. (A) Multivariate ENSO index (MEI), and (B) Pacific Decadal Oscillation (PDO) index from 1900 to March 2015. The black lines are 13-month centered average values. MEI index based on MEI.ext data from 1900 to 1949 (Wolter and Timlin, 2011), and MEI data from 1950 to March 2015 (Wolter and Timlin, 1993, 1998); MEI data downloaded from http://www.esrl.noaa.gov/psd/enso. PDO index data from 1900 to March 2015 (Mantua et al., 1997); PDO data downloaded from http://research.jisao.washington.edu/pdo. Refer to sources and links for details on how the MEI and PDO indexes were computed.

Bromirski et al. (2011) attributes suppression of the ReSL trend along the U.S. west coast since the 1980s (Figure 5) to changes in the wind stress curl associated with the PDO regime shift in the mid-1970s (Figure 6). Recently, Hamlington et al. (2016) noted an apparent PDO shift resulting in higher sea levels along the U.S. west coast over the last few years that could persist, leading to higher rates of sea-level rise, similar to the higher rates in the observational record.

Sea-Level Fingerprints. Changes to the Earth's gravitational and deformational response to mass redistribution between the ocean and glaciers, ice caps and ice sheets (cryosphere) is known as sea-level or static-equilibrium fingerprints. As land ice melts, water enters the ocean raising

GMSL; however, a reduced gravitational pull on the ocean water also results from the decrease in ice mass. The overall net effect of these fingerprints is that ReSL will drop near the melting ice masses and increase proportional to the distance from the ice masses.

Vertical land motion. Vertical land motion (VLM) is associated with tectonics, sediment compaction and/or subsidence, and glacial isostatic adjustment (GIA). GIA is the response of the Earth's surface to the retreat of the ice sheets during the last ice age. Regional and local VLM, such as tectonic land-level changes, can be much larger than those associated with GIA models (Zervas, 2009). Along the U.S. west coast, and in particular the CSZ, researchers have documented interseismic tectonic land-level rates from plate locking that are an order of magnitude greater than the global GIA rate (Mitchell et al., 1994; Burgette et al., 2009). Along the PNW coast, the tectonic land-level changes associated with the CSZ strongly affect regional and local sea-level changes (Komar, 2011).

Regional Sea-Level Rise along the Pacific North West Coast and Humboldt Bay Region

To infer VLM associated with tectonic uplift rates from LSL change at six NOAA tide gauge sites located between Crescent City, CA and Astoria, OR, Burgette et al. (2009) determined an average sea-level rise rate of 2.28 ± 0.20 mm/yr that represents an approximate 20th century ReSL rise rate for the PNW coast along the CSZ. As noted by Burgette et al. (2009), the 2.28 mm/yr ReSL rise rate compared well to the 1950 to 2000 GMSL reconstruction of Church and White (2006), which had trend slopes for grid points offshore of the CSZ of 2.2 ± 0.30 mm/yr. Komar et al. (2011) further assessed the 2.28 mm/yr ReSL rate by comparing LSL rates for the six CSZ tide gauge records to the benchmark and Pacific Northwest Geodetic Array Global Positioning System (GPS) data, and concluded that the rate is reasonable for the PNW coast. Finally, the NRC (2012) study determined an adjusted (for VLM and atmospheric pressure) sea level rise rate of 2.30 mm/yr for the Seattle tide gauge for the 1900 to 2008 period, which is also consistent with the 2.28 mm/yr ReSL rise rate.

The 2.28 mm/yr ReSL rise rate is 0.58 mm/yr greater (34% increase) than the 1901 to 2010 GMSL rate of 1.7 mm/yr (Table 1). This implies that natural climate variability (ENSO and PDO), ocean dynamic processes, and gravitational mass redistribution have produced a greater ReSL rise rate for the PNW coast relative to the GMSL rate for the same general period. The Burgette et al. (2009) rate of 2.28 mm/yr has been used by local researchers (e.g. NHE, 2015a; Patton et al., 2017) to represent historic ReSL rise rates for the Humboldt Bay region.

Past and Present Local Sea-Level Rise

Tide gauges measure local sea-level (LSL) change, which is the combined effects of sea-level change and VLM. The measured LSL change includes the same processes affecting ReSL patterns, and other short-term local processes such as wind waves, tides and hydrodynamic effects. As noted by Zervas (2009), VLM is responsible for most of the differences in LSL trends between regional tide observations. For example, although the Crescent City and North Spit tide

gauges are only separated by 109 km (~68 mi), the LSL trends for these gauges are in opposing directions (Figure 7).

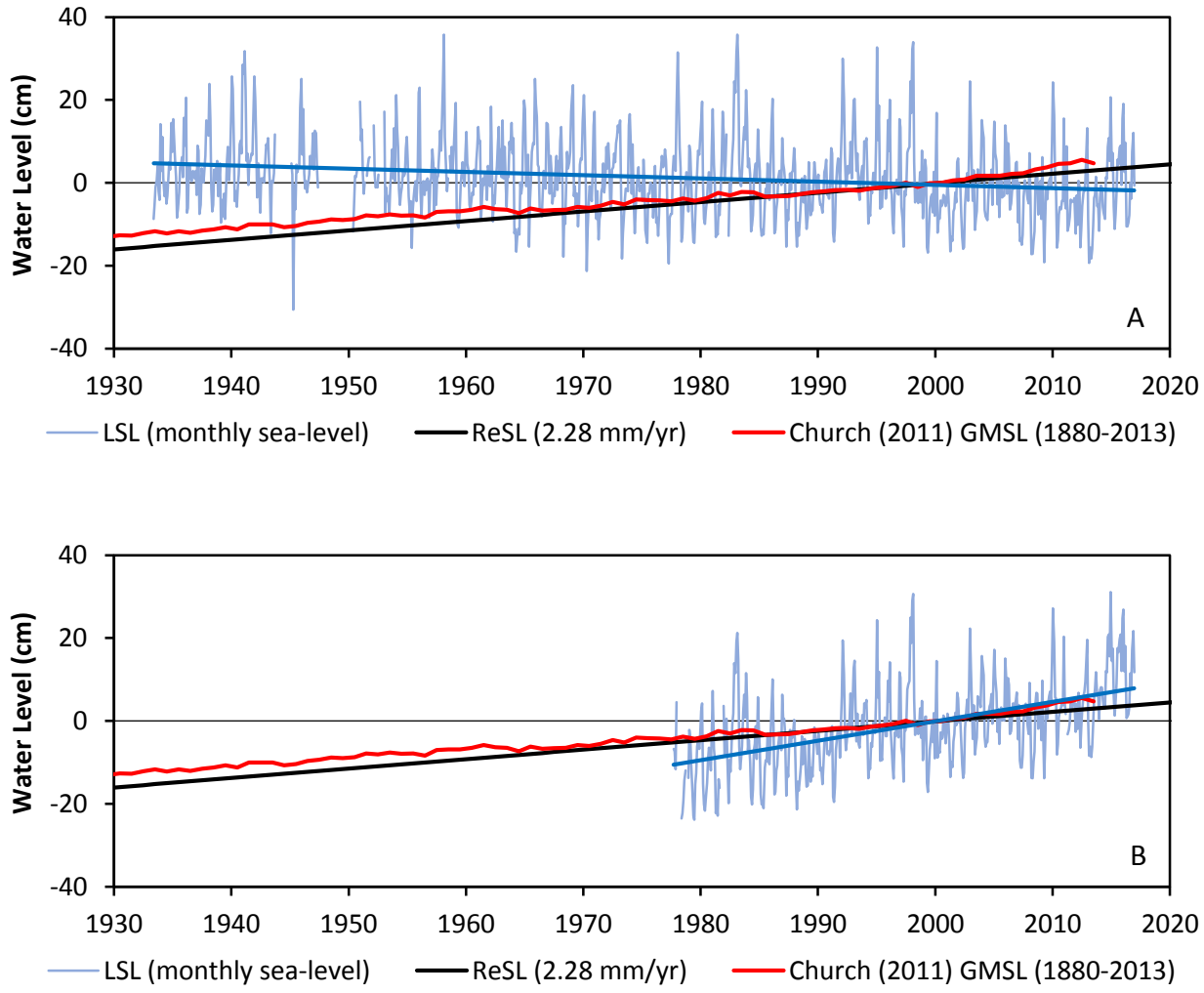

Figure 7. (A) LSL change for Crescent City tide gauge (1933 to 2016). (B) LSL rise for Humboldt Bay North Spit tide gauge (1977 to 2016). LSL changes (light blue lines) are monthly mean values, LSL trends (dark blue lines) are the linear regression on the monthly values, ReSL rise trend (black line) is the Burgette et al. (2009) ReSL rate of 2.28 mm/yr., GMSL rise trend (red line) is the Church and White (2011) reconstruction. All data relative to year 2000 baseline.

The downward LSL trend at Crescent City indicates this section of coast is emerging, with an uplift rate greater than the current GMSL and ReSL rise rates. In contrast, the North Spit LSL trend is greater than the GMSL or ReSL rates, indicating that Humboldt Bay is submergent, and in fact, has the highest LSL rise rate of any tide gauge in California. The relatively large oscillations in monthly LSL values around the trend line are due to short-term weather variability (e.g. storms), natural climate variability (e.g. ENSO and PDO), and the average seasonal cycle.

Local Sea-Level Rise and Vertical Land Motion Rates in the Humboldt Bay Region

The LSL rise rate at North Spit tide gauge is greater than both the GMSL and ReSL rise rates due to land subsidence in and around Humboldt Bay. To better understand how tectonic land motion affects LSL rates in Humboldt Bay, Cascadia Geosciences and partners received funding from the U.S. Fish & Wildlife Service (study plan at http://www.hbv.cascadiageo.org) to utilize tide gauge observations, benchmark level surveys, and GPS data to evaluate tectonic VLM and LSL rates in Humboldt Bay. The tide gauge analysis evaluated water level observations at the NOAA Crescent City tide gauge, and five NOAA tide gauge sites in Humboldt Bay, which include North Spit and four historic gauges located at Mad River Slough, Samoa, Fields Landing, and Hookton Slough (Figure 1, Figure 8).

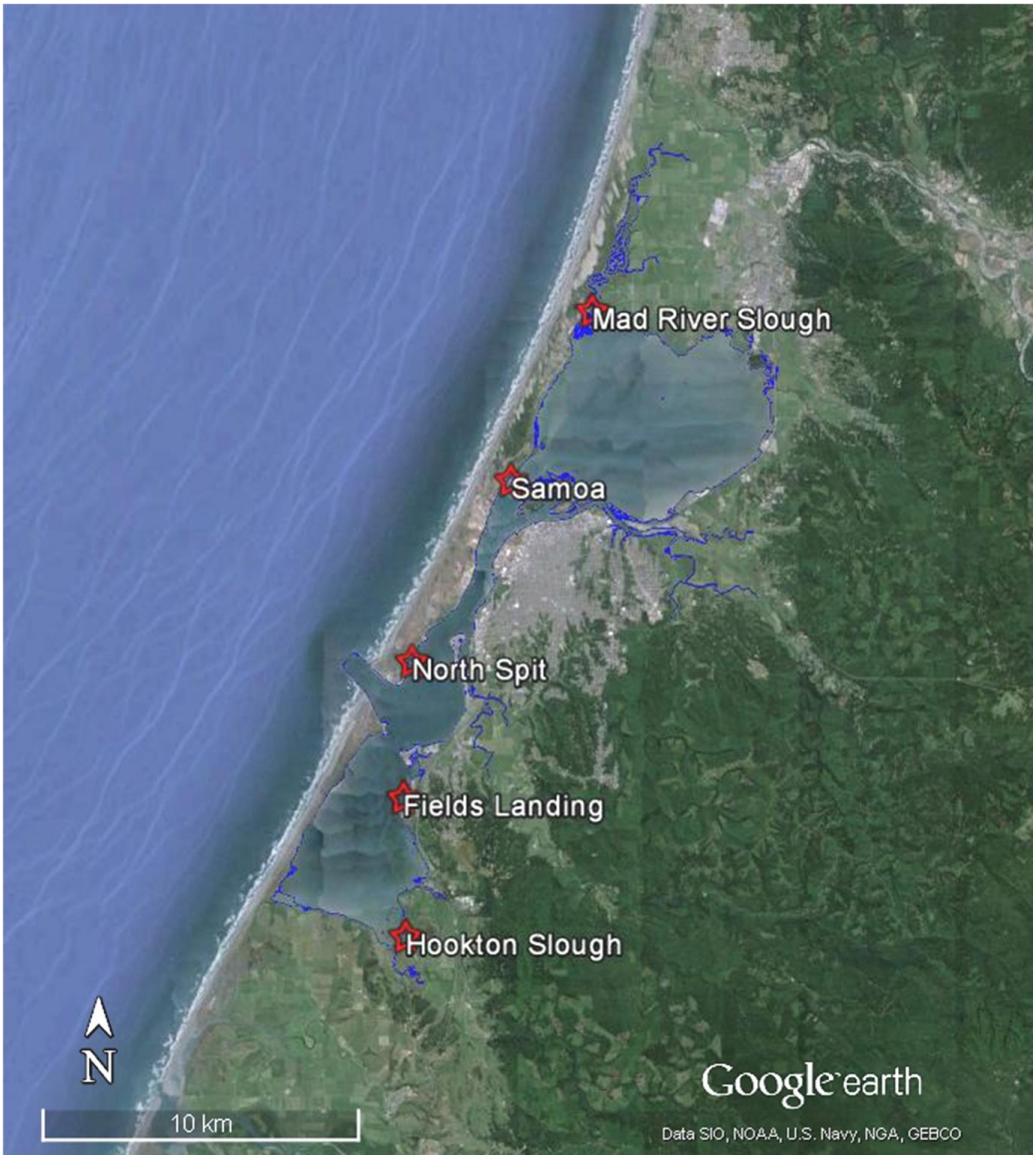

Figure 8. Five NOAA tide gauge locations in Humboldt Bay, and mean high water edge (blue line).

The tide gauge analysis relied on the long-term Crescent City (~84 years) and North Spit (40 years) tide gauges, and the general approach of Mitchell et al. (1994) and Burgette et al. (2009) to determine VLM and LSL rates at the other Humboldt Bay gauges, which all have record lengths less than 30 years and are considered too short to directly determine rates (Zervas, 2009). The analysis also relied on the 20th century ReSL rise rate (2.28 mm/yr) of Burgette et al. (2009).

Recently, NHE (in progress) updated the original VLM and LSL rate estimates of Patton et al. (2017) for the Crescent City and Humboldt Bay tide gauges using a weighted least squares adjustment approach as described by Ghilani (2010) (Table 2, Figure 9). The NHE update work is in progress, but reference to the Patton et al. (2017) work can be made for a general discussion of the tide gauge analysis methods and interpretation of results.

Table 2. Summary of LSL rise and VLM rates for Crescent City and the five Humboldt Bay tide gauges originally developed by Patton et al. (2017), and the weighted least square adjustment values recently developed by NHE (in progress). The weighted least square adjustment provides a mean and standard error (SE) for LSL rise and VLM. Positive VLM rates indicate upward land motion, and negative rates indicate downward motion.

	Patton et al. (2017) Values		**Weighted Least Squares Adjustment (NHE, in progress)**			
Tide Gauge Location	**LSL Rise (mm/yr)**	**VLM (mm/yr)**	**LSL Rise (mm/yr)**	**SE (mm/yr)**	**VLM (mm/yr)**	**SE (mm/yr)**
Crescent City	-0.97	3.25	-0.83	0.07	3.11	0.13
North Spit	4.61	-2.33	4.97	0.27	-2.69	0.25
Mad River Slough	3.39	-1.11	3.32	0.53	-1.04	0.27
Samoa	2.53	-0.25	2.93	1.14	-0.65	0.32
Fields Landing	3.76	-1.48	3.93	0.95	-1.65	0.41
Hookton Slough	5.84	-3.56	5.98	0.81	-3.70	0.41

The north to south down trending VLM gradient controls the LSL rate variation in Humboldt Bay, with the highest rate of VLM in south Humboldt Bay at the Hookton Slough tide gauge. The tectonic deformation in Humboldt Bay increases the LSL rates well above the long-term GMSL and ReSL rates of 1.7 and 2.28 mm/yr, respectively, with both the North Spit and Hookton Slough LSL rates being more than twice the ReSL rate. These higher LSL rise rates indicate that increases in the GMSL and ReSL will affect Humboldt Bay faster than other parts of U.S. west coast; and within the bay, the south end will be affected sooner than the north end.

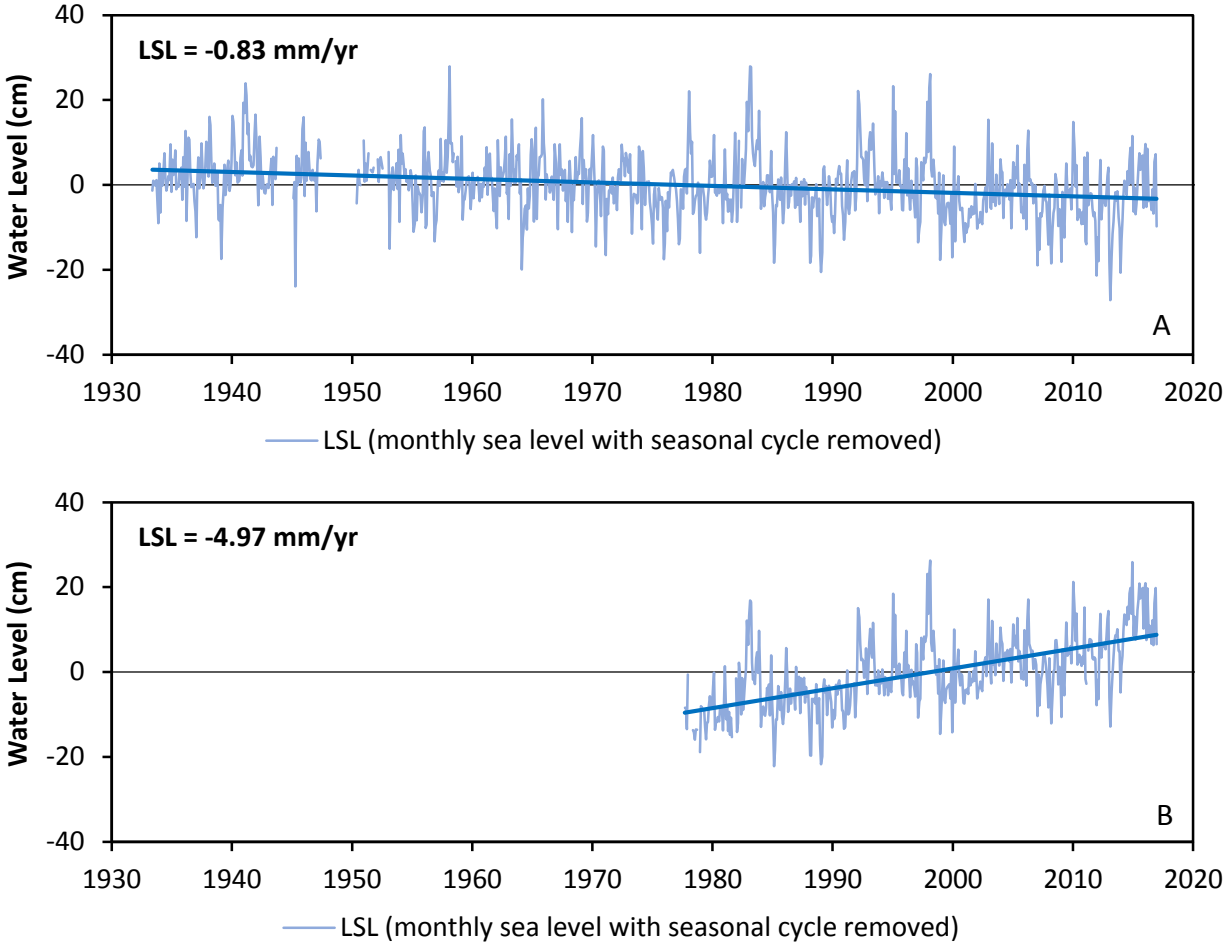

Figure 9. LSL rise trends for (A) Crescent City (1933 to 2016) and (B) North Spit (1977 to 2016) tide gauges using monthly mean sea levels with the average seasonal cycle removed.

Sea-Level Height Variability

Sea-level heights vary due to astronomical tides, storm surge, wind stress effects, changes in barometric pressure, seasonal cycles, and ENSO phases, which results in water levels reaching higher levels over longer time scales (Cayan et al., 2008; Knowles, 2010). Figure 10 shows the hourly water levels for the Crescent City tide gauge for the 1982-83 El Niño years, along with the mean sea level (MSL) and mean higher high water (MHHW) tidal datum, the mean monthly maximum water (MMMW), and the 10- and 100-yr extreme high-water level events.

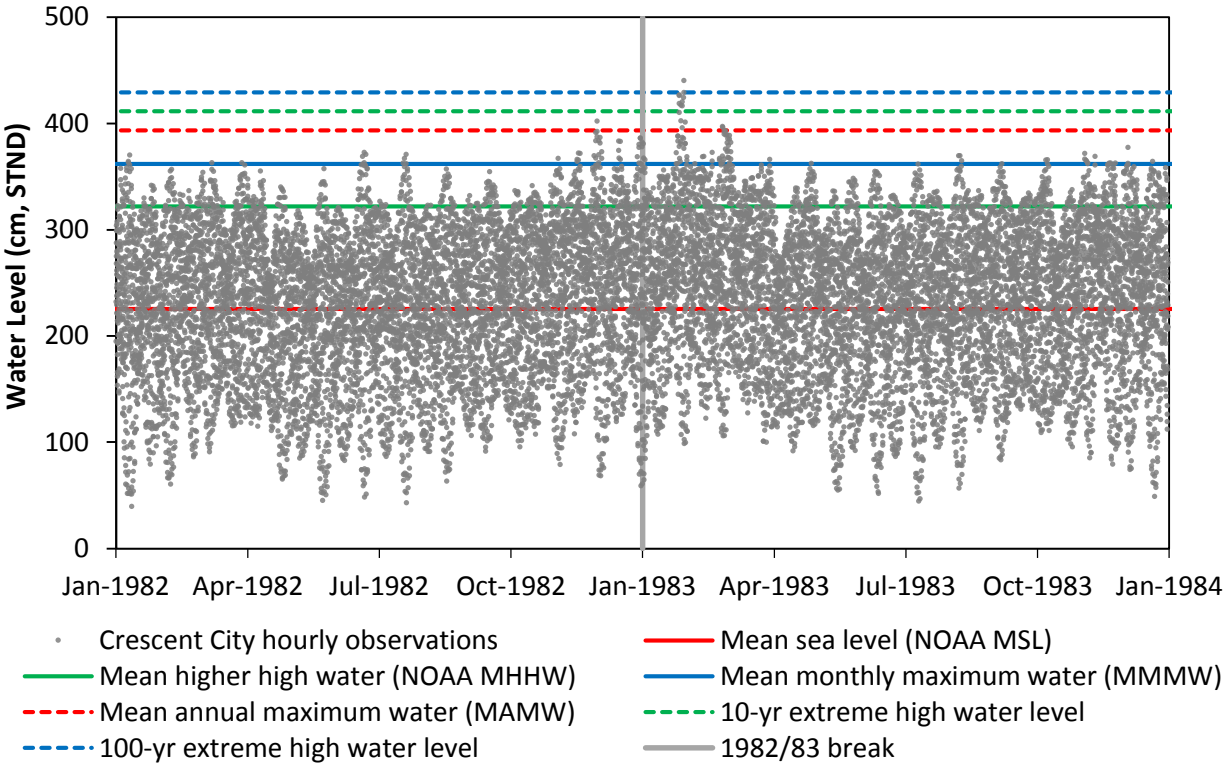

Figure 10. Crescent City tide gauge hourly water levels for 1982-83 El Niño years, with mean sea level (MSL), mean higher high water (MHHW), mean monthly maximum water (MMMW), mean annual maximum water (MAMW), and the 10- and 100-yr extreme high-water level events.

Most coastal damage to the U.S. west coast occurs when storm surge and high waves coincide with high astronomical tides and El Niño events (Cayan et al., 2008; NRC, 2012), which occurred during the winters of 1982-83 and 1997-98. For example, in late January 1983 a large El Niño driven storm coincided with higher than normal astronomical tides, and produced the highest water levels of record at the Crescent City tide gauge on 29 January 1983, exceeding the 100-year extreme exceedance probability event (Figure 10 and Figure 11). The peak hourly water level on 29 January 1983 was 66.2 cm (2.2 ft) higher than the astronomical high tide, and on 26 January 1983, the peak hourly water level was 84.0 cm (2.8 ft) above the astronomical high tide.

It is important to note that sea-level height variability is superimposed onto mean sea level (Cayan et al., 2008). Consequently, as sea-levels rise into the future, the water levels associated with sea-level height variability described above will also increase, and the incidence of extreme high-water levels will become more common (NRC, 2012).

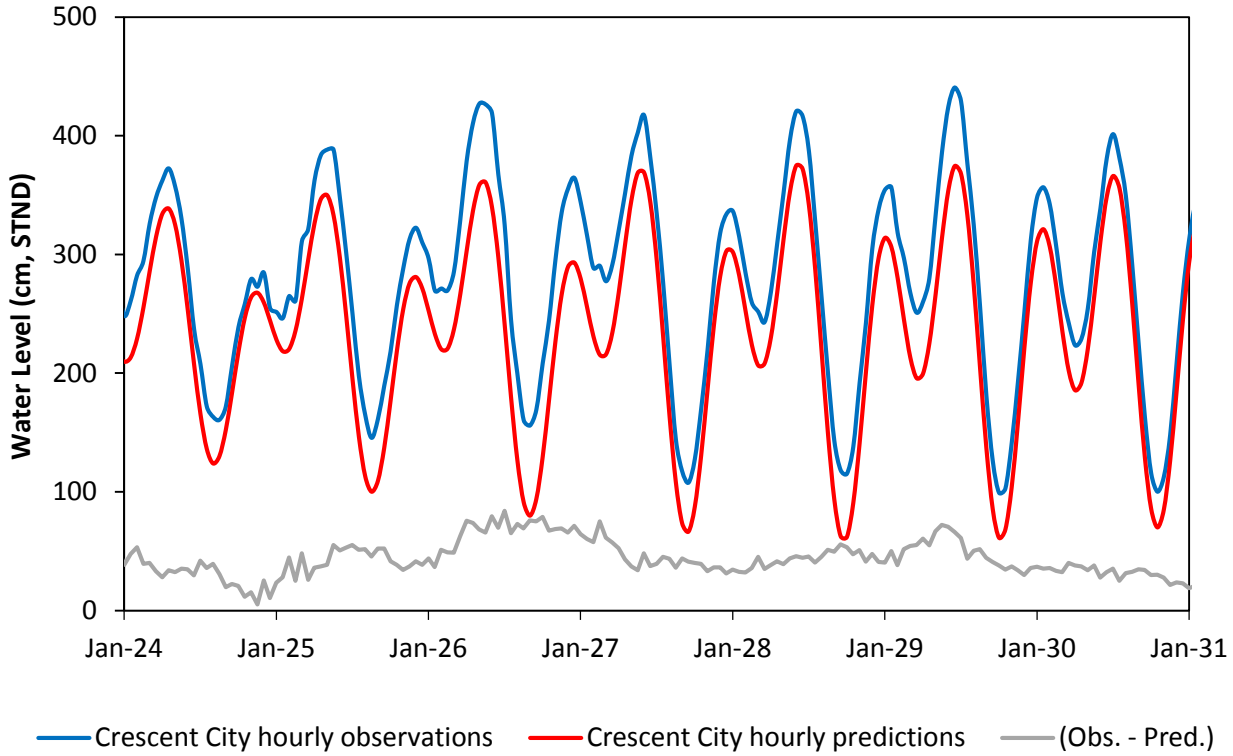

Figure 11. Crescent City tide gauge hourly water levels for January 1983 El Niño year. Blue line is observed water level, green line is astronomical tidal prediction, and grey line is observed minus predicted.

Projections of Sea-Level Rise

Observations provide unequivocal evidence that the climate system is warming and that GMSL has risen over the 20th century (NRC, 2012; IPCC, 2013), but projections of future sea-level rise, including global, regional and local estimates, are necessary to adequately assess and plan for potential impacts to coastal area. Sea-level rise projections generally depend on the understanding of contributions to sea-level change, the response of key geophysical processes, and assumptions regarding future warming of the climate system (NRC, 2012, Church et al., 2013). This section summarizes recent probabilistic projections of GMSL rise and provides probabilistic estimates of LSL rise for the Humboldt Bay region based on the approach of Kopp et al. (2014).

The NRC (2012) report produced regional projections along the U.S. west coast for three scenarios (low, central and high), with the central or "mid-range" projection having the most weight. The NRC projections covered four regions (Seattle, Newport, San Francisco, and Los Angeles) that varied from the global average due to regional oceanic thermal expansion and dynamics, sea level fingerprint effects, and VLM, and represented the most comprehensive regional projections for the U.S. west coast at the time. Since the NRC (2012) report, significant

effort and advances have been made in developing probabilistic projections of GMSL, ReSL and LSL rise (e.g. Church et al., 2013; Kopp et al., 2014; Grinsted et al., 2015).

The recently released OPC sea-level science update for California (Griggs et al., 2017) used the framework of Kopp et al. (2014) to determine probabilistic sea-level rise projections at three representative locations along the California coast (Crescent City, San Francisco, and La Jolla). Unfortunately, none of these locations adequately represent the high rates of LSL rise occurring in the Humboldt Bay region due to tectonically driven VLM.

The approach of Kopp et al. (2014) provides complete probability distributions for GMSL and LSL rise projections at a global network of tide gauge sites under three emission scenarios, RCP 2.6, RCP 4.5 and RCP 8.5 (discussed below). This approach develops individual probability distributions for the sea-level rise components of glacier/ice cap and ice sheet (Greenland and Antarctic) loss with fingerprint affects, oceanic processes (regional dynamic, thermal and steric effects), land water storage, and VLM from process-based model outputs and expert elicitation for the ice sheets. The GMSL and LSL probability distributions were determined by combining 10,000 Latin hypercube samples (a Monte-Carlo approach) from each individual component distribution. The Kopp et al. (2014) GMSL and LSL projections are available for download as supporting information and include the Crescent City and North Spit tide gauges.

The IPCC AR5 adopted a set of greenhouse gas emission scenarios known as Representative Concentration Pathways (RCPs), which represent future emissions and concentrations of greenhouse gases, aerosols, and other climate drivers (Church et al., 2013). The RCPs (RCP 8.5, 6.0, 4.5 and 2.6) represent future radiative forcing by 2100 (e.g. RCP 8.5 is 8.5 W/m^2) and are dependent on various mitigation scenarios including implied policy actions, that have different targets in terms of greenhouse gas emissions and radiative forcing (IPCC, 2013). RCP 8.5 is a very high greenhouse gas emission scenario with high radiative forcing and represents a future where there are no significant efforts to reduce emissions. RCP 2.6 represents an aggressive emission mitigation scenario leading to low radiative forcing and requires net-negative global emissions in the last quarter of the 21st century. RCP 4.5 and 6.0 represent moderate emission mitigation scenarios. Kopp et al. (2014) only provides projections for RCP 2.6, 4.5 and 8.0, and notes that the sea-level rise projections for RCP 6.0 are similar to those for RCP 4.5.

As discussed in Griggs et al. (2017), recent work on Antarctic Ice Sheet modeling has identified modes of ice-sheet instability that could make extreme sea-level rise more likely than indicated in the Kopp et al. (2014) framework. Consequently, the OPC Science Advisory Team included the extreme sea-level rise scenario (GMSL rise of 2.5 m by 2100) of Sweet et al. (2016) with the Kopp et al. (2014) probabilistic projections. Consistent with Griggs et al. (2017), this extreme scenario (called the H++ scenario) was included in the Humboldt Bay region update but was renamed the Ext 2.5 scenario to represent the Sweet et al. (2016) extreme GMSL rise of 2.5 m by 2100. The Sweet et al. (2016) scenario projections are also available as supporting information.

The following sections summarize and provide updated sea-level rise projections for the Humboldt Bay region based on the probabilistic projections of Kopp et al. (2014) and the extreme scenario of Sweet et al. (2017), with the local estimates of VLM by Patton et al. (2017) and NHE (in progress) incorporated into the projections.

Global Mean Sea-Level Rise Projections

The GMSL rise projections of Kopp et al. (2014) for the RCP 8.5, RCP 4.5 and RCP 2.6 emission scenarios (Figure 12, Table 3, Table 4) are provided for consistency and comparison with the LSL projections for the Humboldt Bay region. Table 3 show the component contributions to GMSL rise at 2100 for the median (50% probability) and different probability ranges (e.g. 90 and 99% probabilities). The total GMSL median projections and probabilities for 2030, 2050, 2100, 2150 and 2200 are listed in Table 4, along with the Sweet et al. (2016) Ext 2.5 scenario.

It should be noted that the Ext 2.5 scenario, which has unknown probability, is somewhat consistent with the 99.9% probability of the RCP 8.5 projection (Table 4).

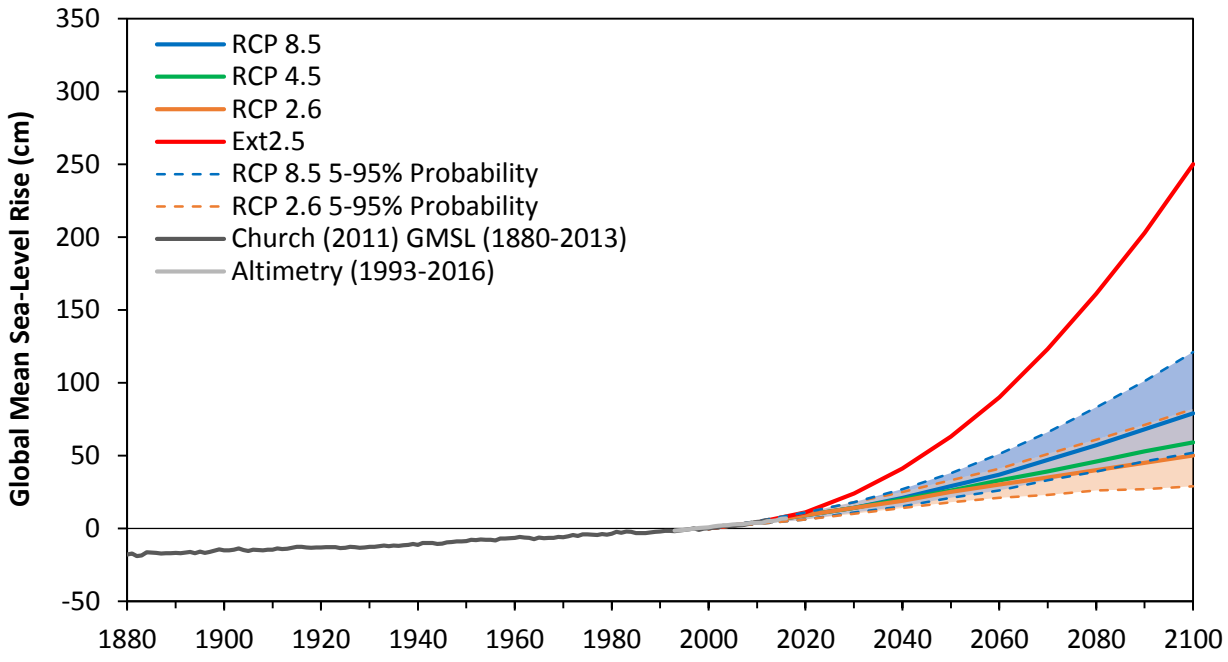

Figure 12. GMSL rise projections for RCP 8.5, RCP 4.5 and RCP 2.6 based on data from Kopp et al. (2014) and the Sweet et al. (2016) extreme scenario of 2.5 m of GMSL rise by 2100 (Ext2.5). The 5 and 95% probabilities are the shaded areas bounded by the dashed lines, and are only shown for RCP 8.5 and RCP 2.6. The reconstructed 1880 to 2013 GMSL curve is from Church et al. (2011). The 1993 to 2016 altimetry data is from Beckley et al. (2010), data downloaded at: https://sealevel.nasa.gov. All data relative to year 2000 baseline.

Table 3. GMSL rise component contributions at year 2100 of Kopp et al. (2014). Sea-level values are cm and ft above year 2000 baseline, probabilities are percent.[1]

	RCP 8.5					RCP 4.5					RCP 2.6				
	50	**17 to 83**	**5 to 95**	**0.5 to 99.5**	**99.9**	**50**	**17 to 83**	**5 to 95**	**0.5 to 99.5**	**99.9**	**50**	**17 to 83**	**5 to 95**	**0.5 to 99.5**	**99.9**
Year 2100 – GMSL rise components (cm)															
GIC	18	14 to 21	11 to 24	7 to 29	< 30	13	10 to 17	7 to 19	3 to 23	< 25	12	9 to 15	7 to 17	3 to 20	< 25
GIS	14	8 to 25	5 to 39	3 to 70	< 95	9	4 to 15	2 to 23	0 to 40	< 55	6	4 to 12	3 to 17	2 to 31	< 45
AIS	4	-8 to 15	-11 to 33	-14 to 91	< 155	5	-5 to 16	-9 to 33	-11 to 88	< 150	6	-4 to 17	-8 to 35	-10 to 93	< 155
TE	37	28 to 46	22 to 52	12 to 62	< 65	26	18 to 34	13 to 40	4 to 48	< 55	19	13 to 26	8 to 31	1 to 38	< 40
LWS	5	3 to 7	2 to 8	0 to 11	< 10	5	3 to 7	2 to 8	0 to 11	< 10	5	3 to 7	2 to 8	0 to 11	< 10
Total	79	62 to 100	52 to 121	39 to 176	< 245	59	45 to 77	36 to 93	24 to 147	< 215	50	37 to 65	29 to 82	19 to 141	< 210
Year 2100 – GMSL rise components (ft)															
GIC	0.6	0.5 to 0.7	0.4 to 0.8	0.2 to 1.0	< 1.0	0.4	0.3 to 0.6	0.2 to 0.6	0.1 to 0.8	< 0.8	0.4	0.3 to 0.5	0.2 to 0.6	0.1 to 0.7	< 0.8
GIS	0.5	0.3 to 0.8	0.2 to 1.3	0.1 to 2.3	< 3.1	0.3	0.1 to 0.5	0.1 to 0.8	0.0 to 1.3	< 1.8	0.2	0.1 to 0.4	0.1 to 0.6	0.1 to 1.0	< 1.5
AIS	0.1	-0.3 to 0.5	-0.4 to 1.1	-0.5 to 3.0	< 5.1	0.2	-0.2 to 0.5	-0.3 to 1.1	-0.4 to 2.9	< 4.9	0.2	-0.1 to 0.6	-0.3 to 1.1	-0.3 to 3.1	< 5.1
TE	1.2	0.9 to 1.5	0.7 to 1.7	0.4 to 2.0	< 2.1	0.9	0.6 to 1.1	0.4 to 1.3	0.1 to 1.6	< 1.8	0.6	0.4 to 0.9	0.3 to 1.0	0.0 to 1.2	< 1.3
LWS	0.2	0.1 to 0.2	0.1 to 0.3	0.0 to 0.4	< 0.3	0.2	0.1 to 0.2	0.1 to 0.3	0.0 to 0.4	< 0.3	0.2	0.1 to 0.2	0.1 to 0.3	0.0 to 0.4	< 0.3
Total	2.6	2.0 to 3.3	1.7 to 4.0	1.3 to 5.8	< 8.0	1.9	1.5 to 2.5	1.2 to 3.1	0.8 to 4.8	< 7.1	1.6	1.2 to 2.1	1.0 to 2.7	0.6 to 4.6	< 6.9

[1]GMSL is global mean sea level; GIC is glaciers and ice caps; GIS is Greenland Ice Sheet; AIS is Antarctic Ice Sheet; TE is thermal expansion; LWS is land water storage; and RCP 8.5, RCP 4.5 and RCP 2.6 are greenhouse gas representative concentration pathways of AR5 (IPCC, 2013).

Table 4. GMSL rise projections of Kopp et al. (2014) and the extreme GMSL scenario (2.5 m of GMSL rise by 2100) of Sweet et al. (2016). Sea-level values are cm and ft above year 2000 baseline; probabilities are percent.[1]

	RCP 8.5					RCP 4.5					RCP 2.6					Ext 2.5
	50	**17 to 83**	**5 to 95**	**0.5 to 99.5**	**99.9**	**50**	**17 to 83**	**5 to 95**	**0.5 to 99.5**	**99.9**	**50**	**17 to 83**	**5 to 95**	**0.5 to 99.5**	**99.9**	**50**
GMSL projections by year (cm)																
2030	14	12 to 17	11 to 18	8 to 21	< 25	14	12 to 16	10 to 18	8 to 20	< 20	14	12 to 16	10 to 18	8 to 20	< 20	24
2050	29	24 to 34	21 to 38	16 to 49	< 60	26	21 to 31	18 to 35	14 to 44	< 55	25	21 to 29	18 to 33	14 to 43	< 55	63
2100	79	62 to 100	52 to 121	39 to 176	< 245	59	45 to 77	36 to 93	24 to 147	< 215	50	37 to 65	29 to 82	19 to 141	< 210	250
2150	130	100 to 180	80 to 230	60 to 370	< 540	90	60 to 130	40 to 170	20 to 310	< 480	70	50 to 110	30 to 150	20 to 290	< 460	550
2200	200	130 to 280	100 to 370	60 to 630	< 950	130	70 to 200	40 to 270	10 to 520	< 830	100	50 to 160	30 to 240	10 to 500	< 810	970
GMSL projections by year (ft)																
2030	0.5	0.4 to 0.6	0.4 to 0.6	0.3 to 0.7	< 0.8	0.5	0.4 to 0.5	0.3 to 0.6	0.3 to 0.7	< 0.7	0.5	0.4 to 0.5	0.3 to 0.6	0.3 to 0.7	< 0.7	0.8
2050	1.0	0.8 to 1.1	0.7 to 1.2	0.5 to 1.6	< 2.0	0.9	0.7 to 1.0	0.6 to 1.1	0.5 to 1.4	< 1.8	0.9	0.7 to 1.0	0.6 to 1.1	0.5 to 1.4	< 1.8	2.1
2100	2.6	2.0 to 3.3	1.7 to 4.0	1.3 to 5.8	< 8.0	1.9	1.5 to 2.5	1.2 to 3.1	0.8 to 4.8	< 7.1	1.9	1.5 to 2.5	1.2 to 3.1	0.8 to 4.8	< 7.1	8.2
2150	4.3	3.3 to 5.9	2.6 to 7.5	2.0 to 12.1	< 17.7	3.0	2.0 to 4.3	1.3 to 5.6	0.7 to 10.2	< 15.7	3.0	2.0 to 4.3	1.3 to 5.6	0.7 to 10.2	< 15.7	18.0
2200	6.6	4.3 to 9.2	3.3 to 12.1	2.0 to 20.7	< 31.2	4.3	2.3 to 6.6	1.3 to 8.9	0.3 to 17.1	< 27.2	4.3	2.3 to 6.6	1.3 to 8.9	0.3 to 17.1	< 27.2	31.8

[1]GMSL is global mean sea level; RCP 8.5, RCP 4.5 and RCP 2.6 are greenhouse gas representative concentration pathways of AR5 (IPCC, 2013); and EXT2.5 is the extreme sea-level rise of 2.5 m of GMSL rise by 2100 of Sweet et al. (2016).

Local Sea-Level Rise Projections for the Humboldt Bay Region

As part of this work, NHE (in progress) updated and/or developed LSL rise probabilistic projections for the RCP 8.5, 4.5 and 2.6 emission scenarios at four sites in the Humboldt Bay region: Crescent City, North Spit, Mad River Slough and Hookton Slough. The three sites in Humboldt Bay (Figure 8) were selected to highlight how the north to south trending VLM gradient affects LSL rise projections.

To provide the LSL rise projections, the Kopp et al. (2014) and Sweet et al. (2016) Ext 2.5 projection data were obtained for the Crescent City and North Spit tide gauges. The VLM contributions to LSL rise for each Kopp et al. (2014) projection were removed (modified Kopp projections) and replaced with the VLM estimates of Patton et al. (2017) as modified by NHE (in progress). Following the same methodology of Kopp et al. (2014), the new VLM probability distributions were determined from 10,000 Latin Hypercube samples assuming a t-distribution with the mean and standard error for the components of the VLM estimates at each site. These VLM probability distributions were combined with the modified Kopp projections to determine LSL rise probabilistic projections for each site. A similar approach was followed for the Ext 2.5 scenario, with the Sweet et al. (2016) projections adjusted with the mean VLM estimate at each site.

For the LSL projections, VLM is configured as a contribution to LSL change. For example, the VLM at North Spit is negative (Table 2) indicating that the ground is moving downward. This downward land motion increases sea-level rise at North Spit, resulting in a positive LSL rise contribution, as reported in the LSL tables. The opposite occurs for Crescent City. Table 5 lists the VLM contributions to LSL change (mean and +/- 2 standard deviations) determined by Kopp et al. (2014) for Crescent City and North Spit, and the NHE (in progress) estimates for these two locations and the Mad River Slough and Hookton Slough sites. The locally generated VLM estimates are higher than those determined by Kopp et al. (2014), which will increase or decrease the updated LSL rates, depending on the site.

Table 5. VLM contributions to LSL change determined by Kopp et al. (2014) and by Patton et al. (2017) and NHE (in progress) used in the updated LSL probability projections for the Humboldt Bay region. VLMs are reported as mean and +/- 2 standard deviations (SD).

	VLM rate as contribution to LSL change (mm/yr)			
	Kopp et al. (2014)		**Patton et al. (2017) and NHE (in progress)**	
Tide Gauge Location	**Mean**	**+/- 2 SD**	**Mean**	**+/- 2 SD**
Crescent City	-2.63	0.30	-3.11	0.27
Mad River Slough			1.04	0.67
North Spit	1.64	0.76	2.69	0.53
Hookton Slough			3.70	1.31

The modified LSL projections for Crescent City and North Spit are shown in Figure 13. The 2100 component contributions to LSL rise for Crescent City, North Spit, Mad River Slough and Hookton Slough are provided in Table 6 for the median (50% probability) and different probability ranges (e.g. 90 and 99% probabilities). The total LSL median projection and probabilities at each site for 2030, 2050, 2100, 2150 and 2200 are listed in Table 7, along with the Sweet et al. (2016) extreme scenario (Ext 2.5).

Findings/Discussion

Comparing the 2100 projections for LSL within the Humboldt Bay region to GMSL (Table 3 and Table 6) show differences between GMSL and LSL rise components, and reveal important regional and local factors that affect LSL change compared to GMSL. Within the Humboldt Bay region oceanic dynamic processes appear to have a limited effect on increasing sea levels beyond GMSL projections, except for small increases for the lower RCPs. Contributions from the glaciers/ice caps and Greenland Ice Sheet are projected to be lower than global averages for all RCPs. The Antarctic Ice Sheet is projected to have only slight increases above the global average for the lower RCPs. However, unlike other portions of the U.S. west coast that are projected to have sea-level rise close to the global average (Kopp et al., 2014), the Humboldt Bay region has LSL projections well above the GMSL projections due to tectonically driven VLM.

Crescent City, which is uplifting, has LSL rise projections (50% probability of 0.42 m, 90% probability of 0.11 to 0.88) that are below GMSL projections (50% probability of 0.79 m, 90% probability of 0.52 to 1.21) under RCP 8.5 by 2100. However, North Spit is subsiding, and has LSL projections (50% value of 1.01 m, 90% probability of 0.69 to 1.46) that are above the GMSL projections by 2100 for RCP 8.5. Likewise, Mad River Slough and Hookton Slough also have LSL projections that are above the global average, with Hookton Slough having the highest rates, due to the north to south trending downward VLMs in Humboldt Bay.

It should be noted that up to 2050, differences between LSL projections are minimal between RCP emission scenarios, and the RCP 8.5 projections can just be used (Kopp et al., 2014; Griggs et al., 2017). After 2050, differences in projections begin to emerge due to emission scenarios.

One final note, large interannual monthly and annual mean sea-level variability as occurs in the Humboldt Bay region (Figure 13) can mask LSL rise over the near term (Kopp et al., 2014). The interannual variability also exceeds the uncertainty in projections (~90% probability) until about 2030 to 2040 for annual mean sea levels, and about 2040 to 2050 for monthly mean sea levels. During these timeframes, the interannual variability, either alone or in combination with the LSL rise projections, should be considered in decision making.

The key finding from the updated probabilistic LSL projections is that the tectonically driven VLM in Humboldt Bay creates the highest LSL rise rates in California. These higher LSL rates indicate that GMSL rise will impact Humboldt Bay faster than other parts of the U.S. west coast; and within the bay, the south end will be impacted sooner than the north end.

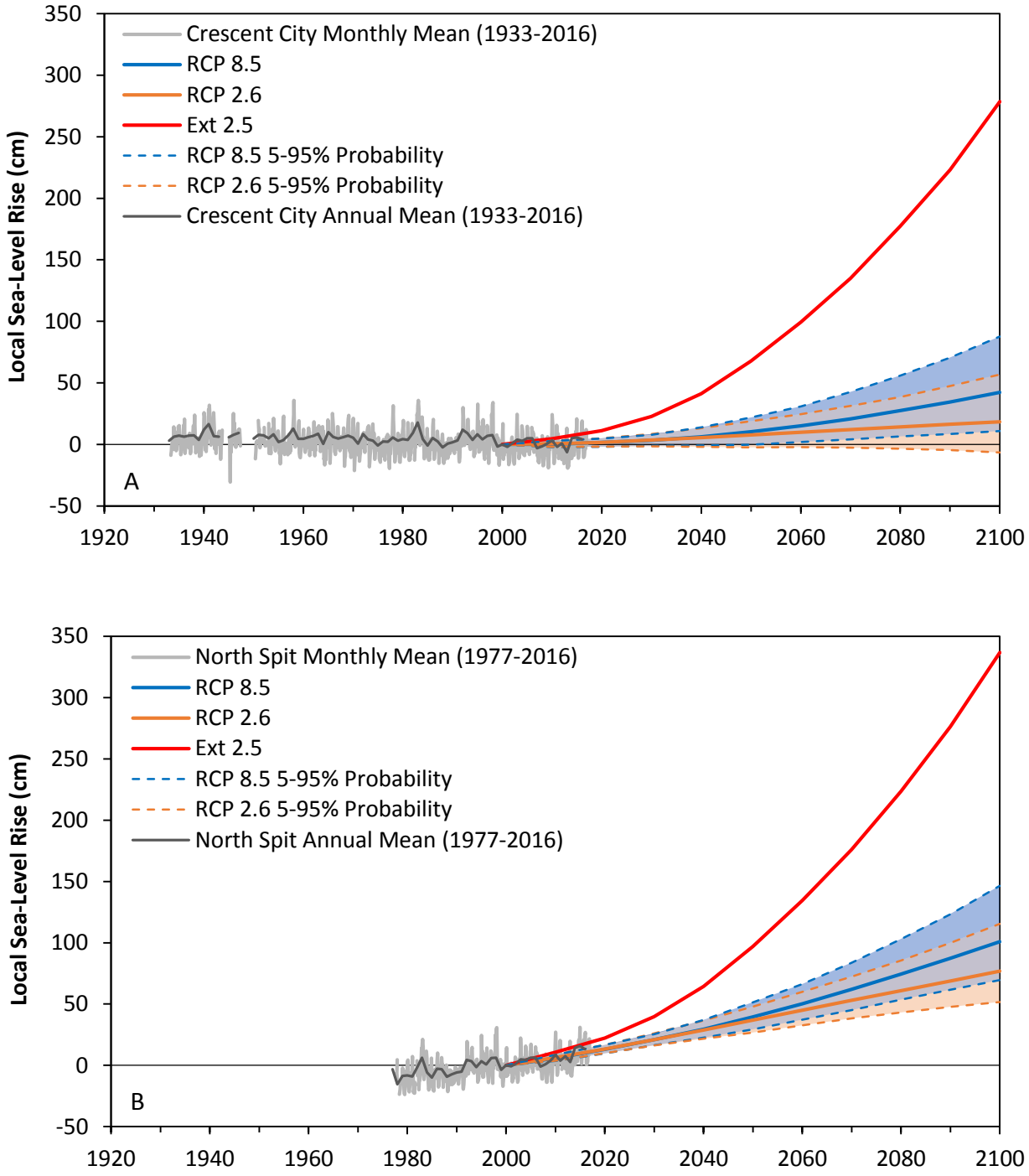

Figure 13. LSL rise projections at Crescent City (A) and North Spit (B) for RCP 8.5 and RCP 2.6 based on data from Kopp et al. (2014), the Sweet et al. (2016) extreme scenario of 2.5 m of GMSL rise by 2100 (Ext 2.5), and VLM contribution to LSL rise by Patton et al. (2017) and NHE (in progress). The 5 and 95 % probabilities are the shaded areas bounded by the dashed lines. The LSL curves are the annual and monthly mean sea levels for the 1933 to 2016 Crescent City data (NOAA 9419750), and the 1977 to 2016 North Spit data (NOAA 9418767), respectively. All data referenced to year 2000 baseline.

Table 6. LSL rise component contributions at year 2100 for Humboldt Bay Region based on data (GIC, GIS, AIS, Ocean and LWS) from Kopp et al. (2014), and VLM contribution to LSL rise by Patton et al. (2017) and NHE (in progress). Sea-level values are cm and ft above year 2000 baseline; probabilities are percent.[1]

	RCP 8.5					RCP 4.5					RCP 2.6				
	50	**17 to 83**	**5 to 95**	**0.5 to 99.5**	**99.9**	**50**	**17 to 83**	**5 to 95**	**0.5 to 99.5**	**99.9**	**50**	**17 to 83**	**5 to 95**	**0.5 to 99.5**	**99.9**
Crescent City, year 2100 – Sea-level rise components (cm)															
GIC	13	10 to 17	8 to 19	5 to 22	< 24	10	7 to 13	5 to 15	3 to 18	< 20	9	6 to 11	5 to 13	2 to 16	< 18
GIS	12	7 to 22	4 to 33	2 to 59	< 81	8	3 to 13	2 to 19	0 to 34	< 46	5	3 to 10	2 to 15	2 to 26	< 36
AIS	4	-8 to 18	-13 to 38	-15 to 110	< 183	6	-6 to 19	-10 to 39	-12 to 106	< 176	7	-4 to 20	-8 to 41	-11 to 112	< 185
Ocean	37	24 to 49	16 to 58	2 to 70	< 77	27	16 to 39	8 to 47	-4 to 59	< 64	22	12 to 32	6 to 39	-5 to 49	< 54
LWS	5	3 to 7	2 to 8	0 to 11	< 12	5	3 to 7	2 to 8	0 to 11	< 12	5	3 to 7	2 to 8	0 to 11	< 12
VLM	-31	-32 to -30	-33 to -29	-35 to -28	< -27	-31	-32 to -30	-33 to -29	-35 to -28	< -27	-31	-32 to -30	-33 to -29	-35 to -28	< -27
Total	42	23 to 65	11 to 88	-6 to 156	< 228	26	9 to 46	-2 to 65	-17 to 133	< 196	18	3 to 37	-7 to 57	-19 to 127	< 197
Mad River Slough, year 2100 – Sea-level rise components (cm)															
GIC	14	11 to 17	8 to 19	5 to 23	< 25	11	8 to 13	6 to 15	3 to 19	< 20	9	7 to 12	5 to 14	2 to 16	< 18
GIS	12	7 to 22	4 to 34	3 to 60	< 82	8	3 to 13	2 to 20	0 to 34	< 47	6	3 to 10	2 to 15	2 to 27	< 37
AIS	4	-8 to 18	-13 to 39	-16 to 110	< 184	6	-6 to 19	-10 to 39	-12 to 107	< 176	7	-4 to 20	-8 to 41	-11 to 112	< 186
Ocean	37	25 to 49	16 to 57	3 to 69	< 75	27	16 to 38	9 to 46	-4 to 58	< 63	22	13 to 31	6 to 38	-5 to 48	< 53
LWS	5	3 to 7	2 to 8	0 to 11	< 12	5	3 to 7	2 to 8	0 to 11	< 12	5	3 to 7	2 to 8	0 to 11	< 12
VLM	10	8 to 13	5 to 16	1 to 20	< 24	10	8 to 13	5 to 16	1 to 20	< 24	10	8 to 13	5 to 16	1 to 20	< 24
Total	84	65 to 107	53 to 130	36 to 198	< 279	68	51 to 88	40 to 108	24 to 174	< 241	60	45 to 79	35 to 99	21 to 169	< 241
North Spit, year 2100 – Sea-level rise components (cm)															
GIC	14	11 to 17	8 to 19	5 to 23	< 25	11	8 to 13	6 to 15	3 to 19	< 20	9	7 to 12	5 to 14	2 to 16	< 18
GIS	12	7 to 22	4 to 34	3 to 60	< 82	8	3 to 13	2 to 20	0 to 34	< 47	6	3 to 10	2 to 15	2 to 27	< 37
AIS	4	-8 to 18	-13 to 39	-16 to 110	< 184	6	-6 to 19	-10 to 39	-12 to 107	< 176	7	-4 to 20	-8 to 41	-11 to 112	< 186
Ocean	37	25 to 49	16 to 57	3 to 69	< 75	27	16 to 38	9 to 46	-4 to 58	< 63	22	13 to 31	6 to 38	-5 to 48	< 53
LWS	5	3 to 7	2 to 8	0 to 11	< 12	5	3 to 7	2 to 8	0 to 11	< 12	5	3 to 7	2 to 8	0 to 11	< 12
VLM	27	24 to 29	23 to 31	20 to 34	< 36	27	24 to 29	23 to 31	20 to 34	< 36	27	24 to 29	23 to 31	20 to 34	< 36
Total	101	82 to 124	69 to 146	53 to 214	< 288	85	67 to 104	56 to 124	41 to 189	< 259	77	62 to 96	52 to 115	38 to 184	< 259
Hookton Slough, year 2100 – Sea-level rise components (cm)															
GIC	14	11 to 17	8 to 19	5 to 23	< 25	11	8 to 13	6 to 15	3 to 19	< 20	9	7 to 12	5 to 14	2 to 16	< 18
GIS	12	7 to 22	4 to 34	3 to 60	< 82	8	3 to 13	2 to 20	0 to 34	< 47	6	3 to 10	2 to 15	2 to 27	< 37
AIS	4	-8 to 18	-13 to 39	-16 to 110	< 184	6	-6 to 19	-10 to 39	-12 to 107	< 176	7	-4 to 20	-8 to 41	-11 to 112	< 186
Ocean	37	25 to 49	16 to 57	3 to 69	< 75	27	16 to 38	9 to 46	-4 to 58	< 63	22	13 to 31	6 to 38	-5 to 48	< 53
LWS	5	3 to 7	2 to 8	0 to 11	< 12	5	3 to 7	2 to 8	0 to 11	< 12	5	3 to 7	2 to 8	0 to 11	< 12
VLM	37	32 to 42	28 to 46	14 to 59	< 75	37	32 to 42	28 to 46	14 to 59	< 75	37	32 to 42	28 to 46	14 to 59	< 75
Total	111	91 to 135	79 to 158	60 to 224	< 293	95	77 to 116	65 to 136	47 to 200	< 266	87	71 to 107	61 to 127	44 to 195	< 266

Table 6. Continued

	RCP 8.5					RCP 4.5					RCP 2.6				
	50	**17 to 83**	**5 to 95**	**0.5 to 99.5**	**99.9**	**50**	**17 to 83**	**5 to 95**	**0.5 to 99.5**	**99.9**	**50**	**17 to 83**	**5 to 95**	**0.5 to 99.5**	**99.9**
Crescent City, year 2100 – Sea-level rise components (ft)															
GIC	0.4	0.3 to 0.6	0.3 to 0.6	0.2 to 0.7	< 0.8	0.3	0.2 to 0.4	0.2 to 0.5	0.1 to 0.6	< 0.7	0.3	0.2 to 0.4	0.2 to 0.4	0.1 to 0.5	< 0.6
GIS	0.4	0.2 to 0.7	0.1 to 1.1	0.1 to 1.9	< 2.7	0.3	0.1 to 0.4	0.1 to 0.6	0.0 to 1.1	< 1.5	0.2	0.1 to 0.3	0.1 to 0.5	0.1 to 0.9	< 1.2
AIS	0.1	-0.3 to 0.6	-0.4 to 1.2	-0.5 to 3.6	< 6.0	0.2	-0.2 to 0.6	-0.3 to 1.3	-0.4 to 3.5	< 5.8	0.2	-0.1 to 0.7	-0.3 to 1.3	-0.3 to 3.7	< 6.1
Ocean	1.2	0.8 to 1.6	0.5 to 1.9	0.2 to 2.3	< 2.5	0.9	0.5 to 1.3	0.3 to 1.5	0.0 to 1.9	< 2.1	0.7	0.4 to 1.0	0.2 to 1.3	-0.1 to 1.6	< 1.8
LWS	0.2	0.1 to 0.2	0.1 to 0.3	0.0 to 0.4	< 0.4	0.2	0.1 to 0.2	0.1 to 0.3	0.0 to 0.4	< 0.4	0.2	0.1 to 0.2	0.1 to 0.3	0.0 to 0.4	< 0.4
VLM	-1.0	-1.1 to -1.0	-1.1 to -0.9	-1.1 to -0.9	< -0.9	-1.0	-1.1 to -1.0	-1.1 to -0.9	-1.1 to -0.9	< -0.9	-1.0	-1.1 to -1.0	-1.1 to -0.9	-1.1 to -0.9	< -0.9
Total	1.4	0.8 to 2.1	0.4 to 2.9	-0.1 to 5.1	< 7.5	0.9	0.3 to 1.5	-0.1 to 2.1	-0.4 to 4.3	< 6.4	0.6	0.1 to 1.2	-0.2 to 1.9	-0.5 to 4.2	< 6.5
Mad River Slough, year 2100 – Sea-level rise components (ft)															
GIC	0.5	0.4 to 0.6	0.3 to 0.6	0.2 to 0.8	< 0.8	0.4	0.3 to 0.4	0.2 to 0.5	0.1 to 0.6	< 0.7	0.3	0.2 to 0.4	0.2 to 0.5	0.1 to 0.5	< 0.6
GIS	0.4	0.2 to 0.7	0.1 to 1.1	0.1 to 2.0	< 2.7	0.3	0.1 to 0.4	0.1 to 0.7	0.0 to 1.1	< 1.5	0.2	0.1 to 0.3	0.1 to 0.5	0.1 to 0.9	< 1.2
AIS	0.1	-0.3 to 0.6	-0.4 to 1.3	-0.5 to 3.6	< 6.0	0.2	-0.2 to 0.6	-0.3 to 1.3	-0.4 to 3.5	< 5.8	0.2	-0.1 to 0.7	-0.3 to 1.3	-0.3 to 3.7	< 6.1
Ocean	1.2	0.8 to 1.6	0.5 to 1.9	0.2 to 2.3	< 2.5	0.9	0.5 to 1.2	0.3 to 1.5	0.0 to 1.9	< 2.1	0.7	0.4 to 1.0	0.2 to 1.2	-0.1 to 1.6	< 1.7
LWS	0.2	0.1 to 0.2	0.1 to 0.3	0.0 to 0.4	< 0.4	0.2	0.1 to 0.2	0.1 to 0.3	0.0 to 0.4	< 0.4	0.2	0.1 to 0.2	0.1 to 0.3	0.0 to 0.4	< 0.4
VLM	0.3	0.2 to 0.4	0.2 to 0.5	0.1 to 0.7	< 0.8	0.3	0.2 to 0.4	0.2 to 0.5	0.1 to 0.7	< 0.8	0.3	0.2 to 0.4	0.2 to 0.5	0.1 to 0.7	< 0.8
Total	2.8	2.1 to 3.5	1.7 to 4.3	1.3 to 6.5	< 9.1	2.2	1.7 to 2.9	1.3 to 3.5	0.9 to 5.7	< 7.9	2.0	1.5 to 2.6	1.1 to 3.3	0.8 to 5.5	< 7.9
North Spit, year 2100 – Sea-level rise components (ft)															
GIC	0.5	0.4 to 0.6	0.3 to 0.6	0.2 to 0.8	< 0.8	0.4	0.3 to 0.4	0.2 to 0.5	0.1 to 0.6	< 0.7	0.3	0.2 to 0.4	0.2 to 0.5	0.1 to 0.5	< 0.6
GIS	0.4	0.2 to 0.7	0.1 to 1.1	0.1 to 2.0	< 2.7	0.3	0.1 to 0.4	0.1 to 0.7	0.0 to 1.1	< 1.5	0.2	0.1 to 0.3	0.1 to 0.5	0.1 to 0.9	< 1.2
AIS	0.1	-0.3 to 0.6	-0.4 to 1.3	-0.5 to 3.6	< 6.0	0.2	-0.2 to 0.6	-0.3 to 1.3	-0.4 to 3.5	< 5.8	0.2	-0.1 to 0.7	-0.3 to 1.3	-0.3 to 3.7	< 6.1
Ocean	1.2	0.8 to 1.6	0.5 to 1.9	0.2 to 2.3	< 2.5	0.9	0.5 to 1.2	0.3 to 1.5	0.0 to 1.9	< 2.1	0.7	0.4 to 1.0	0.2 to 1.2	-0.1 to 1.6	< 1.7
LWS	0.2	0.1 to 0.2	0.1 to 0.3	0.0 to 0.4	< 0.4	0.2	0.1 to 0.2	0.1 to 0.3	0.0 to 0.4	< 0.4	0.2	0.1 to 0.2	0.1 to 0.3	0.0 to 0.4	< 0.4
VLM	0.9	0.8 to 1.0	0.7 to 1.0	0.7 to 1.1	< 1.2	0.9	0.8 to 1.0	0.7 to 1.0	0.7 to 1.1	< 1.2	0.9	0.8 to 1.0	0.7 to 1.0	0.7 to 1.1	< 1.2
Total	3.3	2.7 to 4.1	2.3 to 4.8	1.9 to 7.0	< 9.5	2.8	2.2 to 3.4	1.8 to 4.1	1.5 to 6.2	< 8.5	2.5	2.0 to 3.1	1.7 to 3.8	1.4 to 6.1	< 8.5
Hookton Slough, year 2100 – Sea-level rise components (ft)															
GIC	0.5	0.4 to 0.6	0.3 to 0.6	0.2 to 0.8	< 0.8	0.4	0.3 to 0.4	0.2 to 0.5	0.1 to 0.6	< 0.7	0.3	0.2 to 0.4	0.2 to 0.5	0.1 to 0.5	< 0.6
GIS	0.4	0.2 to 0.7	0.1 to 1.1	0.1 to 2.0	< 2.7	0.3	0.1 to 0.4	0.1 to 0.7	0.0 to 1.1	< 1.5	0.2	0.1 to 0.3	0.1 to 0.5	0.1 to 0.9	< 1.2
AIS	0.1	-0.3 to 0.6	-0.4 to 1.3	-0.5 to 3.6	< 6.0	0.2	-0.2 to 0.6	-0.3 to 1.3	-0.4 to 3.5	< 5.8	0.2	-0.1 to 0.7	-0.3 to 1.3	-0.3 to 3.7	< 6.1
Ocean	1.2	0.8 to 1.6	0.5 to 1.9	0.2 to 2.3	< 2.5	0.9	0.5 to 1.2	0.3 to 1.5	0.0 to 1.9	< 2.1	0.7	0.4 to 1.0	0.2 to 1.2	-0.1 to 1.6	< 1.7
LWS	0.2	0.1 to 0.2	0.1 to 0.3	0.0 to 0.4	< 0.4	0.2	0.1 to 0.2	0.1 to 0.3	0.0 to 0.4	< 0.4	0.2	0.1 to 0.2	0.1 to 0.3	0.0 to 0.4	< 0.4
VLM	1.2	1.1 to 1.4	0.9 to 1.5	0.6 to 1.9	< 2.5	1.2	1.1 to 1.4	0.9 to 1.5	0.6 to 1.9	< 2.5	1.2	1.1 to 1.4	0.9 to 1.5	0.6 to 1.9	< 2.5
Total	3.6	3.0 to 4.4	2.6 to 5.2	2.1 to 7.3	< 9.6	3.1	2.5 to 3.8	2.1 to 4.5	1.7 to 6.6	< 8.7	2.9	2.3 to 3.5	2.0 to 4.2	1.6 to 6.4	< 8.7

[1]LSL is local sea level; VLM is vertical land motion contribution to LSL; GIC is glaciers and ice caps; GIS is Greenland Ice Sheet; AIS is Antarctic Ice Sheet; Ocean is ocean thermal, steric and dynamic contribution; LWS is land water storage; RCP 8.5, RCP 4.5 and RCP 2.6 are greenhouse gas representative concentration pathways of AR5 (IPCC, 2013).

Table 7. LSL rise projections for Humboldt Bay Region based on data from Kopp et al. (2014), the extreme GMSL scenario (2.5 m of GMSL rise by 2100) of Sweet et al. (2016), and VLM contribution to LSL rise by Patton et al. (2017) and NHE (in progress). Sea-level values are cm and ft above year 2000 baseline; probabilities are percent.[1]

	RCP 8.5					RCP 4.5					RCP 2.6					Ext 2.5
	50	**17 to 83**	**5 to 95**	**0.5 to 99.5**	**99.9**	**50**	**17 to 83**	**5 to 95**	**0.5 to 99.5**	**99.9**	**50**	**17 to 83**	**5 to 95**	**0.5 to 99.5**	**99.9**	**50**
Crescent City LSL rise projections by year (cm)																
2030	3	1 to 6	-1 to 8	-4 to 11	< 13	3	0 to 6	-3 to 9	-6 to 13	< 15	3	1 to 6	-1 to 8	-4 to 12	< 14	23
2050	10	4 to 17	0 to 22	-6 to 33	< 51	9	3 to 15	-2 to 20	-8 to 31	< 46	8	2 to 14	-2 to 19	-9 to 30	< 46	68
2100	42	23 to 65	11 to 88	-6 to 156	< 228	26	9 to 46	-2 to 65	-17 to 133	< 196	18	3 to 37	-7 to 57	-19 to 127	< 197	279
2150	75	40 to 123	20 to 176	-2 to 338	< 508	43	10 to 85	-10 to 131	-35 to 289	< 455	25	-4 to 62	-17 to 112	-31 to 288	< 462	620
2200	118	54 to 206	19 to 304	-20 to 600	< 916	62	3 to 135	-29 to 219	-68 to 516	< 822	34	-18 to 102	-41 to 194	-62 to 511	< 826	1062
Mad River Slough LSL rise projections by year (cm)																
2030	16	13 to 19	11 to 21	9 to 24	< 27	16	12 to 19	10 to 22	6 to 26	< 28	16	13 to 19	11 to 21	8 to 25	< 28	35
2050	31	25 to 38	21 to 43	15 to 54	< 75	29	23 to 36	19 to 41	13 to 51	< 68	28	23 to 35	18 to 40	12 to 51	< 67	89
2100	84	65 to 107	53 to 130	36 to 198	< 279	68	51 to 88	40 to 108	24 to 174	< 241	60	45 to 79	35 to 99	21 to 169	< 241	320
2150	139	103 to 187	83 to 240	61 to 402	< 574	106	72 to 148	53 to 194	28 to 355	< 522	88	59 to 126	45 to 174	30 to 347	< 530	685
2200	203	138 to 292	103 to 391	64 to 692	< 1009	146	86 to 220	55 to 304	17 to 600	< 913	118	65 to 187	42 to 277	19 to 596	< 918	1149
North Spit LSL rise projections by year (cm)																
2030	21	18 to 23	16 to 25	14 to 29	< 31	21	17 to 24	15 to 26	12 to 30	< 33	21	18 to 24	16 to 26	13 to 29	< 32	40
2050	40	33 to 46	29 to 51	24 to 62	< 81	38	32 to 44	28 to 49	22 to 60	< 76	37	31 to 43	27 to 48	21 to 60	< 75	97
2100	101	82 to 124	69 to 146	53 to 214	< 288	85	67 to 104	56 to 124	41 to 189	< 259	77	62 to 96	52 to 115	38 to 184	< 259	337
2150	163	128 to 211	107 to 266	85 to 424	< 601	131	97 to 172	78 to 219	53 to 375	< 549	112	84 to 150	70 to 200	55 to 371	< 554	710
2200	236	171 to 323	135 to 425	97 to 724	< 1044	179	120 to 252	88 to 338	49 to 633	< 948	151	99 to 219	76 to 311	52 to 629	< 953	1182
Hookton Slough LSL rise projections by year (cm)																
2030	24	21 to 27	19 to 29	15 to 33	< 38	24	20 to 27	17 to 30	13 to 35	< 38	24	21 to 27	19 to 30	15 to 34	< 38	43
2050	45	38 to 52	34 to 57	26 to 69	< 85	43	36 to 50	32 to 55	24 to 67	< 83	42	35 to 49	31 to 54	24 to 66	< 82	102
2100	111	91 to 135	79 to 158	60 to 224	< 293	95	77 to 116	65 to 136	47 to 200	< 266	87	71 to 107	61 to 127	44 to 195	< 266	347
2150	179	142 to 227	121 to 282	96 to 441	< 630	146	112 to 189	92 to 237	63 to 395	< 560	127	99 to 167	84 to 218	65 to 388	< 566	725
2200	257	191 to 345	155 to 447	111 to 739	< 1059	199	140 to 274	107 to 363	64 to 655	< 962	171	119 to 240	94 to 334	65 to 652	< 967	1202

Table 7. Continued

	RCP 8.5					RCP 4.5					RCP 2.6					Ext 2.5
	50	**17 to 83**	**5 to 95**	**0.5 to 99.5**	**99.9**	**50**	**17 to 83**	**5 to 95**	**0.5 to 99.5**	**99.9**	**50**	**17 to 83**	**5 to 95**	**0.5 to 99.5**	**99.9**	**50**
Crescent City LSL rise projections by year (ft)																
2030	0.1	0.0 to 0.2	0.0 to 0.3	-0.1 to 0.4	< 0.4	0.1	0.0 to 0.2	-0.1 to 0.3	-0.2 to 0.4	< 0.5	0.1	0.0 to 0.2	0.0 to 0.3	-0.1 to 0.4	< 0.5	0.7
2050	0.3	0.1 to 0.6	0.0 to 0.7	-0.1 to 1.1	< 1.7	0.3	0.1 to 0.5	-0.1 to 0.7	-0.2 to 1.0	< 1.5	0.3	0.1 to 0.5	-0.1 to 0.6	-0.2 to 1.0	< 1.5	2.2
2100	1.4	0.8 to 2.1	0.4 to 2.9	-0.1 to 5.1	< 7.5	0.9	0.3 to 1.5	-0.1 to 2.1	-0.4 to 4.3	< 6.4	0.6	0.1 to 1.2	-0.2 to 1.9	-0.5 to 4.2	< 6.5	9.1
2150	2.5	1.3 to 4.0	0.7 to 5.8	0.1 to 11.1	< 16.7	1.4	0.3 to 2.8	-0.3 to 4.3	-0.9 to 9.5	< 14.9	0.8	-0.1 to 2.0	-0.5 to 3.7	-0.9 to 9.4	< 15.2	20.4
2200	3.9	1.8 to 6.7	0.6 to 10.0	-0.3 to 19.7	< 30.0	2.0	0.1 to 4.4	-0.9 to 7.2	-1.9 to 16.9	< 27.0	1.1	-0.6 to 3.3	-1.3 to 6.4	-1.9 to 16.8	< 27.1	34.8
Mad River Slough LSL rise projections by year (ft)																
2030	0.5	0.4 to 0.6	0.4 to 0.7	0.3 to 0.8	< 0.9	0.5	0.4 to 0.6	0.3 to 0.7	0.2 to 0.8	< 0.9	0.5	0.4 to 0.6	0.4 to 0.7	0.3 to 0.8	< 0.9	1.1
2050	1.0	0.8 to 1.2	0.7 to 1.4	0.6 to 1.8	< 2.4	1.0	0.8 to 1.2	0.6 to 1.3	0.5 to 1.7	< 2.2	0.9	0.7 to 1.1	0.6 to 1.3	0.5 to 1.7	< 2.2	2.9
2100	2.8	2.1 to 3.5	1.7 to 4.3	1.3 to 6.5	< 9.1	2.2	1.7 to 2.9	1.3 to 3.5	0.9 to 5.7	< 7.9	2.0	1.5 to 2.6	1.1 to 3.3	0.8 to 5.5	< 7.9	10.5
2150	4.6	3.4 to 6.1	2.7 to 7.9	2.2 to 13.2	< 18.8	3.5	2.4 to 4.9	1.7 to 6.4	1.1 to 11.6	< 17.1	2.9	1.9 to 4.1	1.5 to 5.7	1.1 to 11.4	< 17.4	22.5
2200	6.7	4.5 to 9.6	3.4 to 12.8	2.4 to 22.7	< 33.1	4.8	2.8 to 7.2	1.8 to 10.0	0.9 to 19.7	< 29.9	3.9	2.1 to 6.1	1.4 to 9.1	0.8 to 19.6	< 30.1	37.7
North Spit LSL rise projections by year (ft)																
2030	0.7	0.6 to 0.8	0.5 to 0.8	0.5 to 0.9	< 1.0	0.7	0.6 to 0.8	0.5 to 0.9	0.4 to 1.0	< 1.1	0.7	0.6 to 0.8	0.5 to 0.9	0.5 to 1.0	< 1.1	1.3
2050	1.3	1.1 to 1.5	1.0 to 1.7	0.8 to 2.0	< 2.6	1.2	1.0 to 1.4	0.9 to 1.6	0.8 to 2.0	< 2.5	1.2	1.0 to 1.4	0.9 to 1.6	0.7 to 2.0	< 2.5	3.2
2100	3.3	2.7 to 4.1	2.3 to 4.8	1.9 to 7.0	< 9.5	2.8	2.2 to 3.4	1.8 to 4.1	1.5 to 6.2	< 8.5	2.5	2.0 to 3.1	1.7 to 3.8	1.4 to 6.1	< 8.5	11.0
2150	5.4	4.2 to 6.9	3.5 to 8.7	3.0 to 13.9	< 19.7	4.3	3.2 to 5.7	2.6 to 7.2	1.9 to 12.3	< 18.0	3.7	2.8 to 4.9	2.3 to 6.6	1.9 to 12.2	< 18.2	23.3
2200	7.7	5.6 to 10.6	4.4 to 13.9	3.4 to 23.8	< 34.3	5.9	3.9 to 8.3	2.9 to 11.1	1.9 to 20.8	< 31.1	5.0	3.2 to 7.2	2.5 to 10.2	1.9 to 20.6	< 31.3	38.8
Hookton Slough LSL rise projections by year (ft)																
2030	0.8	0.7 to 0.9	0.6 to 1.0	0.5 to 1.1	< 1.3	0.8	0.7 to 0.9	0.6 to 1.0	0.5 to 1.1	< 1.3	0.8	0.7 to 0.9	0.6 to 1.0	0.5 to 1.1	< 1.2	1.4
2050	1.5	1.2 to 1.7	1.1 to 1.9	0.9 to 2.3	< 2.8	1.4	1.2 to 1.6	1.0 to 1.8	0.9 to 2.2	< 2.7	1.4	1.2 to 1.6	1.0 to 1.8	0.9 to 2.2	< 2.7	3.3
2100	3.6	3.0 to 4.4	2.6 to 5.2	2.1 to 7.3	< 9.6	3.1	2.5 to 3.8	2.1 to 4.5	1.7 to 6.6	< 8.7	2.9	2.3 to 3.5	2.0 to 4.2	1.6 to 6.4	< 8.7	11.4
2150	5.9	4.7 to 7.5	4.0 to 9.3	3.4 to 14.5	< 20.7	4.8	3.7 to 6.2	3.0 to 7.8	2.3 to 13.0	< 18.4	4.2	3.2 to 5.5	2.7 to 7.2	2.3 to 12.7	< 18.6	23.8
2200	8.4	6.3 to 11.3	5.1 to 14.7	4.0 to 24.3	< 34.8	6.5	4.6 to 9.0	3.5 to 11.9	2.4 to 21.5	< 31.6	5.6	3.9 to 7.9	3.1 to 11.0	2.4 to 21.4	< 31.7	39.4

[1]LSL is local sea level; RCP 8.5, RCP 4.5 and RCP 2.6 are greenhouse gas representative concentration pathways of AR5 (IPCC, 2013); and Ext 2.5 is the extreme 2.5 m of GMSL rise by 2100 of Sweet et al. (2016).

City of Arcata Local Sea-Level Rise Data and Information

This section provides data and information specific to the northern portion of Humboldt Bay (North Bay) that is more applicable for the City of Arcata sea-level rise planning and decision-making efforts. Information presented in this section relies on the modeling and analysis work conducted by NHE for the Humboldt Bay: Sea Level Rise, Hydrodynamic Modeling, and Inundation Vulnerability Mapping report (NHE, 2015a). Modeling and analysis results were used to produce inundation vulnerability maps of areas surrounding Humboldt Bay vulnerable to inundation from existing and future sea levels, along with bay-wide spatial data of average water levels of mean higher high water (MHHW), mean monthly maximum water (MMMW), and mean annual maximum water (MAMW), and extreme high-water level events (e.g. 100-yr flood level).

As part of the modeling and mapping work, a two-dimensional hydrodynamic model was developed and used to predict water levels within the existing shoreline of Humboldt Bay for five sea-level rise scenarios: year 2012 existing sea levels and half-meter sea-level rise increments of 0.5, 1.0, 1.5 and 2.0 m. The hydrodynamic model was forced by a 100-yr long hourly sea-level height series. Each model simulation produced 100-years of 15-minute predicted water levels at each model grid in the bay. Estimates of average high-water levels (e.g. MHHW) and annual exceedance probabilities of extreme high-water levels (e.g. 100-yr flood) were determined at each model grid cell for each of the five sea-level rise scenarios.

It should be noted that the open ocean boundary condition for the model accounts for sea-level height variability from astronomical tides, and the effects of wind, sea-level pressure, and El Niño variability (NHE, 2015a). However, the effects of internally generated wind waves on predicted water levels in Humboldt Bay were not assessed. The extreme high-water level elevations presented in the NHE (2015a) report do not represent what FEMA defines as the 1% annual base flood elevation, which includes wave effects. The water levels presented in the NHE (2015a) report correspond more closely to what FEMA defines as still water elevations.

In 2015, with funding from the City of Arcata, NHE (2015b) developed an Excel application that allows users to extract estimated average water levels and annual exceedance probabilities of extreme high-water levels at any hydrodynamic model grid cell in Humboldt Bay. The application also allows the user to interpolate a specific sea-level rise value, within the range of sea-level rise scenarios (year 2012 to 2.0 m), from the extracted grid cell water levels using spline interpolation. This application is used here to provide water-level elevations specific to the City of Arcata for the updated probabilistic LSL rise projections.

Sea-Level Rise Projections

The probabilistic LSL rise projections for Mad River Slough (Table 6 and Table 7) and the VLM estimate for Mad River Slough of 1.04 ± 0.67 mm/yr (Table 2) are the most appropriate for the City of Arcata to use in their sea-level rise planning and decision making efforts.

The half-meter sea-level rise scenarios (0.5, 1.0, 1.5 and 2.0 m) modeled in the NHE (2015a) study were not tied to any sea-level rise projection timeline. However, the scenarios were developed in the context of published sea-level rise projections (e.g. NRC, 2012) available at the time of that work, which resulted in the 2.0 m maximum scenario. Figure 14 shows the five sea-level rise scenarios compared to the probabilistic LSL rise projections for Mad River Slough for RCP 8.5, 4.5 and 2.6 (50% probability, and 90% probabilities for RCP 8.5 and 2.6). The half-meter sea-level rise scenarios cover most of the LSL projections range for Mad River Slough, except for the Ext 2.5 scenario which crosses the 2.0 m scenario line around 2080. Review of Table 7 also shows that the 99.9% probability value (279 cm) at 2100 for RCP 8.5 also exceeds the 2.0 m scenario. As noted by Griggs et al. (2017), sea-level rise is not currently following the Ext 2.5 scenario or extreme probabilistic projections; however, current modeling and research indicates the possibility of extreme sea-level rise by the end of this century.

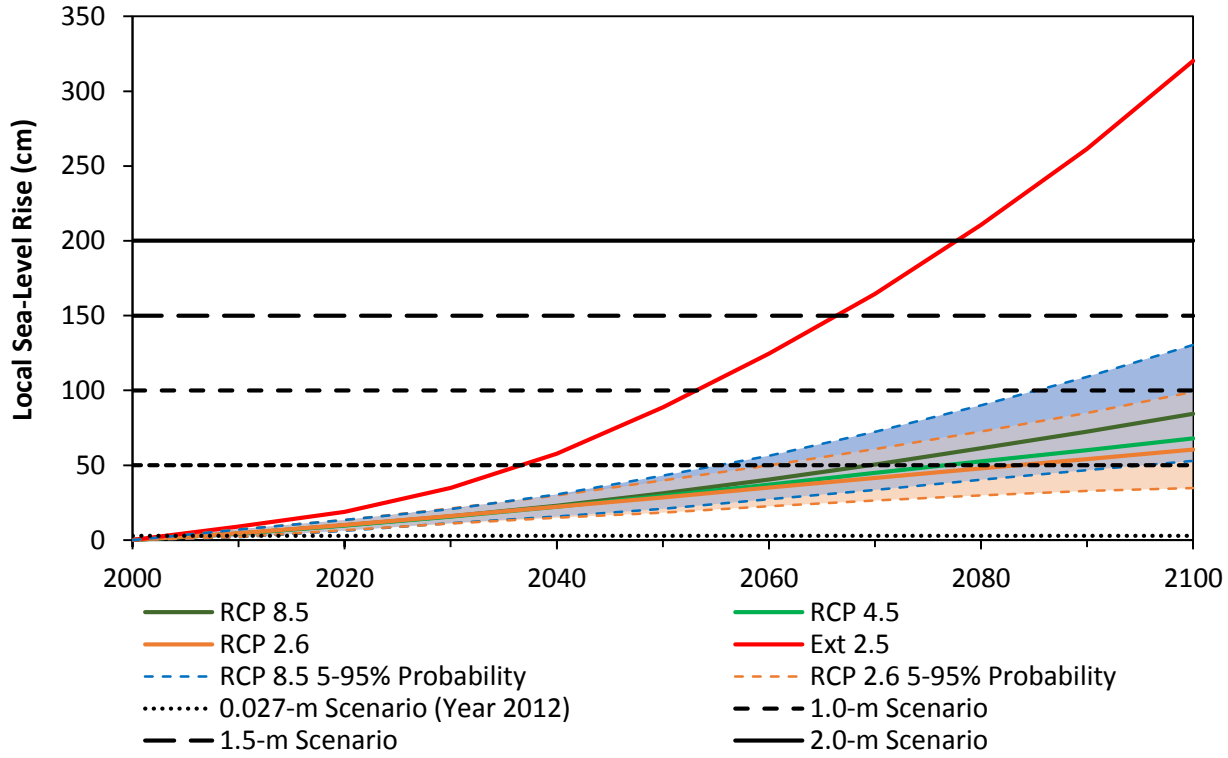

Figure 14. Humboldt Bay half-meter sea-level rise scenarios modeled in the NHE (2015a) study compared to the LSL rise projections at Mad River Slough for RCP 8.5, RCP 4.5 and RCP 2.6. The 5 and 95 % probabilities for RCP 8.5 and RCP 2.6 are the shaded areas bounded by the dashed lines. All data is referenced to year 2000 baseline.

Predicted Water-Level Elevations at the Arcata Marsh & Wildlife Sanctuary

Water-level elevations at the Arcata Marsh & Wildlife Sanctuary for the five sea-level rise scenarios (year 2012 existing sea levels and 0.5, 1.0, 1.5 and 2.0 m) were generated from model

predictions that specifically apply to the City of Arcata (Table 8). It should be noted that modeled water-levels varied less than 1-cm between Jacoby Creek and Mad River Slough, except for MHHW estimates which varied up to 100 cm depending on whether the grid cell was on a mud flat or tidal wetland. Results presented here were extracted from a grid cell over mud flat near the Arcata Marsh & Wildlife Sanctuary and can be used to represent water levels at most locations of interest for the City of Arcata. However, if MHHW elevations near a specific tidal wetland is of interest, it may be necessary to extract that water level from the nearest tidal wetland grid cell, depending on the need.

To support more specific sea-level rise planning and decision making efforts for the City of Arcata, the Excel application was used to provide the 50% probability (median) and 95% probability water-level elevations at 2030, 2050 and 2100 for RCP 8.5 (Table 9) at the Arcata Marsh & Wildlife Sanctuary. As discussed earlier, the large interannual monthly and annual mean sea-level variability that occurs in the Humboldt Bay region (Figure 1) can mask near term LSL rise. For the 2030 and 2050 projections in Table 9, it will be necessary to consider the effects of interannual variability, either alone, or in combination with the LSL projections.

Effects of LSL Rise on Predicted Water-Levels

The LSL projections estimate how mean sea levels will change as GMSL increases. However, extreme sea-level events are the cause of most damage to the California coast (Cayan et al., 2008; NRC, 2012), making it critical to understand the effects of sea-level rise on extreme events. Figure 15, which shows predicted water levels at the Arcata Marsh & Wildlife Sanctuary, demonstrates the importance of considering extreme events when planning for sea-level rise, compared to using average tidal levels such as MHHW. For example, the 100-yr extreme event is approximately 2 meters higher than mean sea level, 1 meter higher than MHHW, and 0.4 meters higher than MAMW. Furthermore, the 2-yr extreme event is approximately equal to MAMW, and the 1-yr event is only slightly greater than MMMW, showing how, on average, the more frequent extreme events are related to average water levels in the bay near the City of Arcata.

Figure 16 shows the predicted extreme high-water level events for year 2012 existing sea levels, and the half-meter increment sea-level rise scenarios of 0.5, 1.0, 1.5 and 2.0-m relative to year 2000 at the Arcata Marsh & Wildlife Sanctuary. Over time, sea-level rise increases the extreme high-water events. Furthermore, as sea-levels rise, the frequency of inundation of fixed water-levels increases. For example, the 1.1-yr extreme event under the 0.5-m sea-level rise scenario relative to year 2000, is approximately equal to the 100-yr event today, which is consistent with other parts of Humboldt Bay (NHE, 2015a) and in San Francisco Bay (Knowles, 2009).

To better understand how sea-level rise effects water levels, a frequency analysis was conducted for the predicted water levels at the Arcata Marsh & Wildlife Sanctuary that assessed the number

Table 8. Tidal levels and annual extreme high-water level probability estimates near Arcata Marsh & Wildlife Sanctuary for year 2012 existing sea levels and the 0.5, 1.0, 1.5 and 2.0-m sea-level rise scenarios (NHE, 2015a). Water levels are from 2D model predictions (NHE, 2015a). Water-level elevations are in cm and ft (NAVD88).[1]

Parameter	Return Interval (yr)	Year 2012	0.5 m Scenario	1.0 m Scenario	1.5 m Scenario	2.0 m Scenario
Elevations in cm (NAVD88)						
MHHW		216	264	315	364	414
MMMW		257	305	357	407	457
MAMW		288	336	387	437	486
1.01-yr	1.01	264	313	364	414	463
1.1-yr	1.1	272	321	372	421	471
1.5-yr	1.5	281	330	380	430	480
2-yr	2	286	335	385	435	485
5-yr	5	298	347	397	446	496
10-yr	10	305	354	404	453	503
25-yr	25	314	362	412	462	511
50-yr	50	320	368	418	467	517
100-yr	100	325	374	424	473	523
500-yr	500	337	385	435	484	535
Elevations in ft (NAVD88)						
MHHW		7.1	8.7	10.3	12.0	13.6
MMMW		8.4	10.0	11.7	13.3	15.0
MAMW		9.4	11.0	12.7	14.3	15.9
1.01-yr	1.01	8.7	10.3	11.9	13.6	15.2
1.1-yr	1.1	8.9	10.5	12.2	13.8	15.5
1.5-yr	1.5	9.2	10.8	12.5	14.1	15.7
2-yr	2	9.4	11.0	12.6	14.3	15.9
5-yr	5	9.8	11.4	13.0	14.6	16.3
10-yr	10	10.0	11.6	13.2	14.9	16.5
25-yr	25	10.3	11.9	13.5	15.1	16.8
50-yr	50	10.5	12.1	13.7	15.3	17.0
100-yr	100	10.7	12.3	13.9	15.5	17.2
500-yr	500	11.0	12.6	14.3	15.9	17.5

[1]MHHW is mean higher high water, MMMW is mean monthly maximum water, MAMW is mean annual maximum water.

Table 9. Tidal levels and annual extreme high-water level probability estimates near Arcata Marsh & Wildlife Sanctuary for updated probabilistic LSL projections for 2030, 2050 and 2100 for RCP 8.5. Water levels are provided for 50% (median) and 95% probabilities. Water levels are interpolated from 2D model predictions (NHE, 2015a). Water-level elevations are in cm and ft (NAVD88).[1]

Parameter	Return Interval (yr)	2030		2050		2100	
		50%	95%	50%	95%	50%	95%
Elevations in cm (NAVD88)							
MHHW		229	234	245	257	299	345
MMMW		270	275	286	298	341	387
MAMW		301	306	317	329	371	417
1.01-yr	1.01	278	282	294	306	348	394
1.1-yr	1.1	286	290	302	314	356	402
1.5-yr	1.5	295	300	311	323	365	411
2-yr	2	300	305	316	328	370	416
5-yr	5	312	317	327	340	381	427
10-yr	10	319	324	335	347	388	434
25-yr	25	328	332	343	355	397	442
50-yr	50	333	338	349	361	403	448
100-yr	100	339	344	355	367	408	454
500-yr	500	350	355	366	378	420	465
Elevations in ft (NAVD88)							
MHHW		7.5	7.7	8.0	8.4	9.8	11.3
MMMW		8.9	9.0	9.4	9.8	11.2	12.7
MAMW		9.9	10.0	10.4	10.8	12.2	13.7
1.01-yr	1.01	9.1	9.3	9.6	10.0	11.4	12.9
1.1-yr	1.1	9.4	9.5	9.9	10.3	11.7	13.2
1.5-yr	1.5	9.7	9.8	10.2	10.6	12.0	13.5
2-yr	2	9.8	10.0	10.4	10.8	12.1	13.6
5-yr	5	10.2	10.4	10.7	11.1	12.5	14.0
10-yr	10	10.5	10.6	11.0	11.4	12.7	14.2
25-yr	25	10.7	10.9	11.3	11.7	13.0	14.5
50-yr	50	10.9	11.1	11.5	11.9	13.2	14.7
100-yr	100	11.1	11.3	11.6	12.0	13.4	14.9
500-yr	500	11.5	11.7	12.0	12.4	13.8	15.3

[1]MHHW is mean higher high water, MMMW is mean monthly maximum water, MAMW is mean annual maximum water.

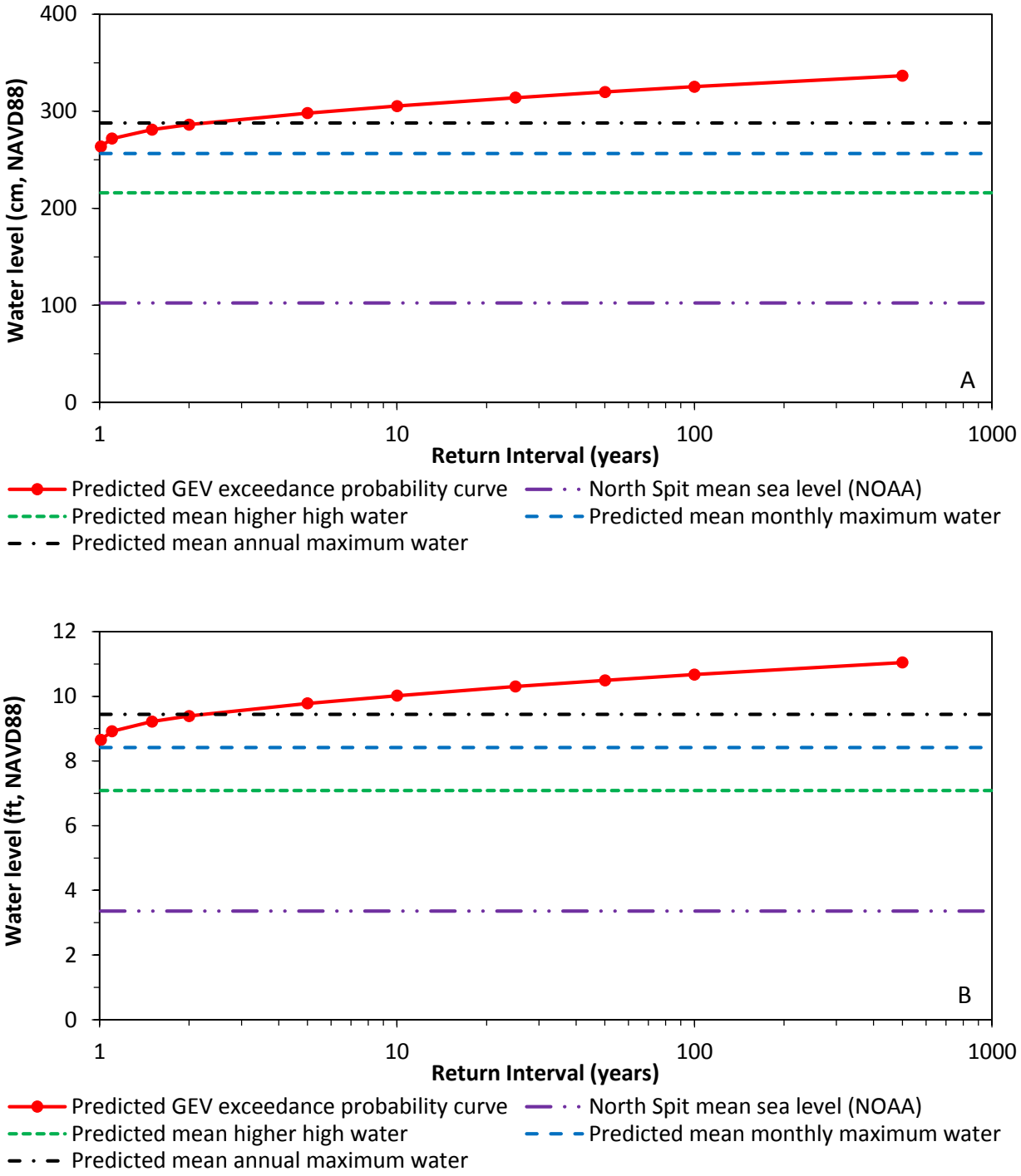

Figure 15. Humboldt Bay year 2012 existing sea-level scenario water levels near Arcata Marsh & Wildlife Sanctuary in units of cm (A) and ft (B). The generalized extreme value (GEV) probability curve, mean higher high water, mean monthly maximum water, and mean annual maximum water are from 2D model predictions (NHE, 2015a). Mean sea level is for North Spit tide gauge (1983-2001 National Tidal Datum Epoch). Water-level elevations in cm and ft (NAVD88).

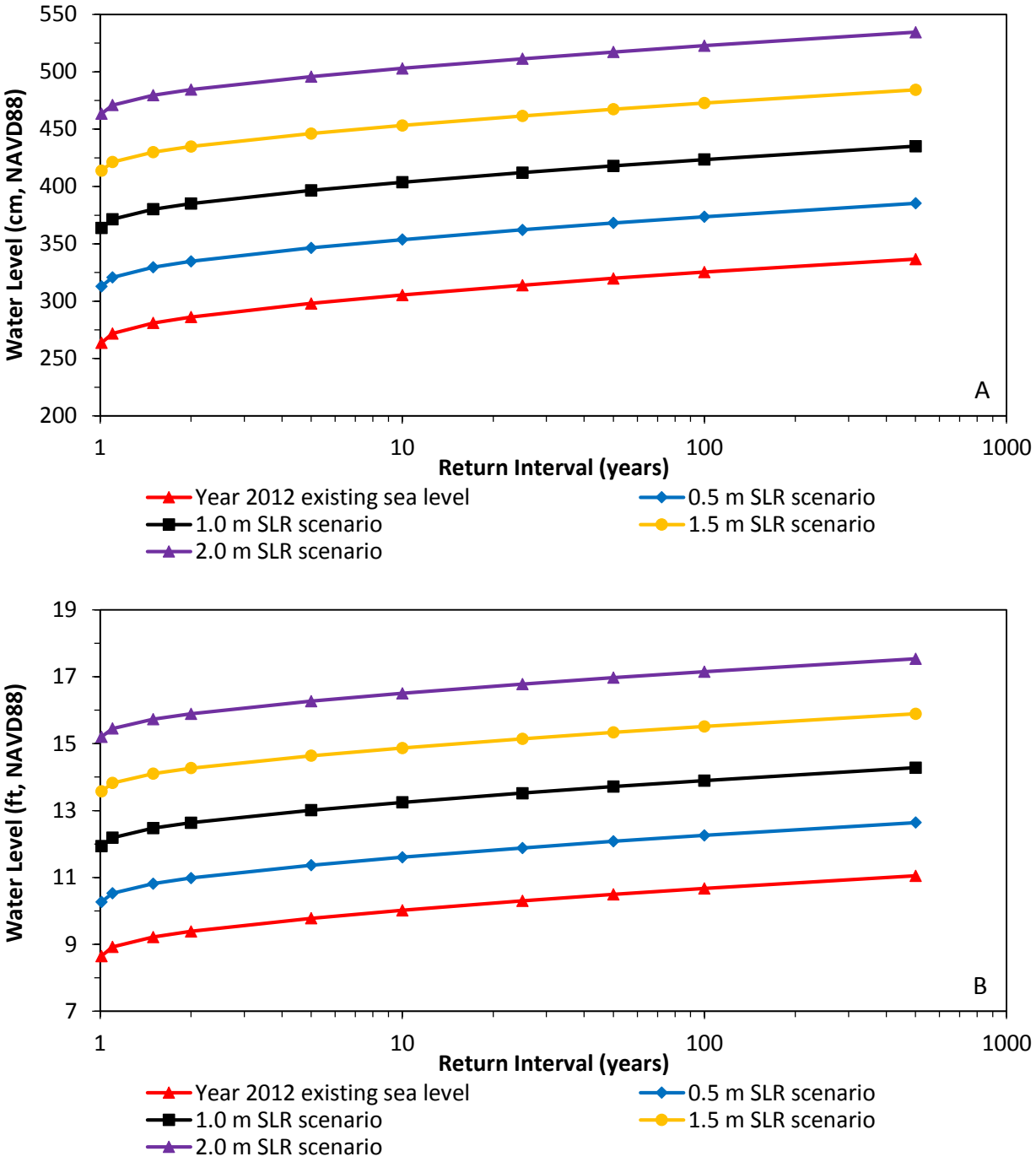

Figure 16. Annual extreme high-water level exceedance probability curves near Arcata Marsh & Wildlife Sanctuary in units of cm (A) and ft (B) for year 2012 existing sea levels and the 0.5, 1.0, 1.5 and 2.0-m sea-level rise scenarios relative to year 2000. All generalized extreme value (GEV) exceedance probability curves are from the 2D model predictions (NHE, 2015a). Water-level elevations are in cm and ft (NAVD88).

of days water levels exceeded year 2012 values for each half-meter sea-level rise scenario (Table 10). As sea-levels increase, the number of days that a current extreme water level is exceeded also increases. For example, the 2-year extreme event (approximately equivalent to MAMW) increases from about 1 day per year today to 67 days per year with 0.5 meters of LSL rise, to 319 days per year for 1 meter of LSL rise, and daily at 1.5 meters. For the 100-yr event, which occurs well below 1 day per year today, will be exceeded 6 days per year with 0.5 meters of LSL rise, about 118 days per year with 1 meter of LSL rise, and will be exceeded almost daily after 1.5 meters of LSL rise.

Table 10. Modeled water-level exceedances above year 2012 base levels near Arcata Marsh & Wildlife Sanctuary for year 2012 existing sea levels and the 0.5, 1.0, 1.5 and 2.0-m sea-level rise scenarios (NHE, 2015a). Water levels are from 2D model predictions (NHE, 2015a). Water-level elevations in cm and ft (NAVD88).[1]

Year 2012		Number of days that Year 2012 base value is exceeded				
Return Interval (yr)	Base Value (cm, NAVD88)	Year 2012	0.5 m Scenario	1.0 m Scenario	1.5 m Scenario	2.0 m Scenario
1.1	272	5	130	351	365	365
1.5	281	2	87	334	365	365
2 (~MAMW)	286	1	67	319	365	365
5	298	0	32	270	365	365
10	305	0	18	231	363	365
25	314	0	9	180	360	365
50	320	0	6	146	354	365
100	325	0	3	118	346	365

To help put this into perspective, since 1912 Humboldt Bay has seen approximately 50 cm of sea-level rise using the North Spit LSL rise rate of 5.0 mm/yr applied over 100 years. Therefore, what was a 100-yr extreme event in 1912 is today about the 1-yr event, or about the monthly average high tide (Figure 15). Using the Hookton Slough LSL rate of 6.0 mm/yr, it would only take approximately 83 years for the 100-yr event to equal the 1-yr event. For Mad River Slough, it would take about 150 years due to the lower LSL rise rate of 3.3 mm/yr. This helps to explain why many Humboldt Bay levees are currently so vulnerable to overtopping by high water level events (Laird, 2013), as many of the bay's levees were constructed in the early 1900s.

Sea-Level Rise Effects on Groundwater and Drainage (An Overview)

The focus of most sea-level rise research, and vulnerability and planning studies has been on the impacts of inundation from rising sea levels and higher storm surge. Groundwater inundation and emergence, or the increase in water table elevation and corresponding decrease in vadose zone thickness, also threatens low-lying coastal communities as sea-levels rise (Walter et al., 2016; Bjerklie et al., 2012; Hoover et al., 2017). Limited research or consideration has been given to

the effect that rising sea-levels will have on groundwater levels, and likewise the impact that elevated groundwater levels will have on coastal communities. The purpose of this section is to provide a brief overview of sea-level rise effects on groundwater and drainage, and to illustrate, based on existing literature, how rising groundwater levels could affect low lying areas in the City of Arcata.

A common assumption in many groundwater assessments is that the groundwater elevation at the ocean edge is at mean sea level (Turner et al., 1997). However, research has shown that the action of tidal oscillations, waves and wave runup can cause fluctuating groundwater levels and a net super-elevation (increase) of the groundwater surface above mean sea level at the ocean boundary in unconfined coastal aquifers (Turner et al., 1997; Rotzoll and El-Kadi, 2008; Monachesi and Guarracino, 2011; Maréchal, n.d.). Similar to considerations for interannual monthly and annual sea-level variability, the effects of elevated groundwater levels above mean sea level will also need to be considered for sea-level rise planning.

Studies, although somewhat limited, have been carried out to analyze the effects of sea-level rise on groundwater elevations in coastal environments and communities. For example, Rotzoll and Fletcher (2012) estimated inundation in Honolulu, HI, and showed that the areal extents of predicted inundation more than doubled when groundwater inundation was combined with the effects of direct sea-level inundation alone. Habel (2016), using a quasi three-dimensional groundwater flow model (MODFLOW) showed that a 1-meter increase in sea level resulted in continuous or episodic flooding throughout most of the study area in Honolulu, HI.

Analyses regarding the effects of sea-level rise on groundwater levels specific to the Arcata-area were carried out by Willis (2014) and Hoover et al. (2017). Willis (2014), used the USGS SUTRA (Saturated-Unsaturated Transport) model to develop a conceptual numerical groundwater model to analyze the potential effects of sea-level rise on the water table in a representative two-dimensional cross-section of the Eureka-Arcata coastal plain (Figure 17). Results of the conceptual model indicate that sea-level rise could increase the degree of saltwater intrusion, and shift the location of the maximum hydraulic head westward (towards the ocean), with more pronounced effects occurring with greater degrees of sea-level rise (Figure 17). Furthermore, the effects of increased groundwater extraction rates and/or decreased recharge rates would increase the degree of saltwater intrusion within the aquifer. Willis (2014) emphasized that the model was a conceptual simulation model, and was not fully calibrated or validated, due to data and budget limitations. It was recommended that additional data collection and studies be carried out to more accurately assess the effects of sea-level rise on groundwater levels within the Eureka-Arcata Plain.

Hoover et al. (2017) assessed the spatial effects of sea-level rise on groundwater emergence in a low-lying area of Arcata (same general area as Willis (2014) study) and two other California

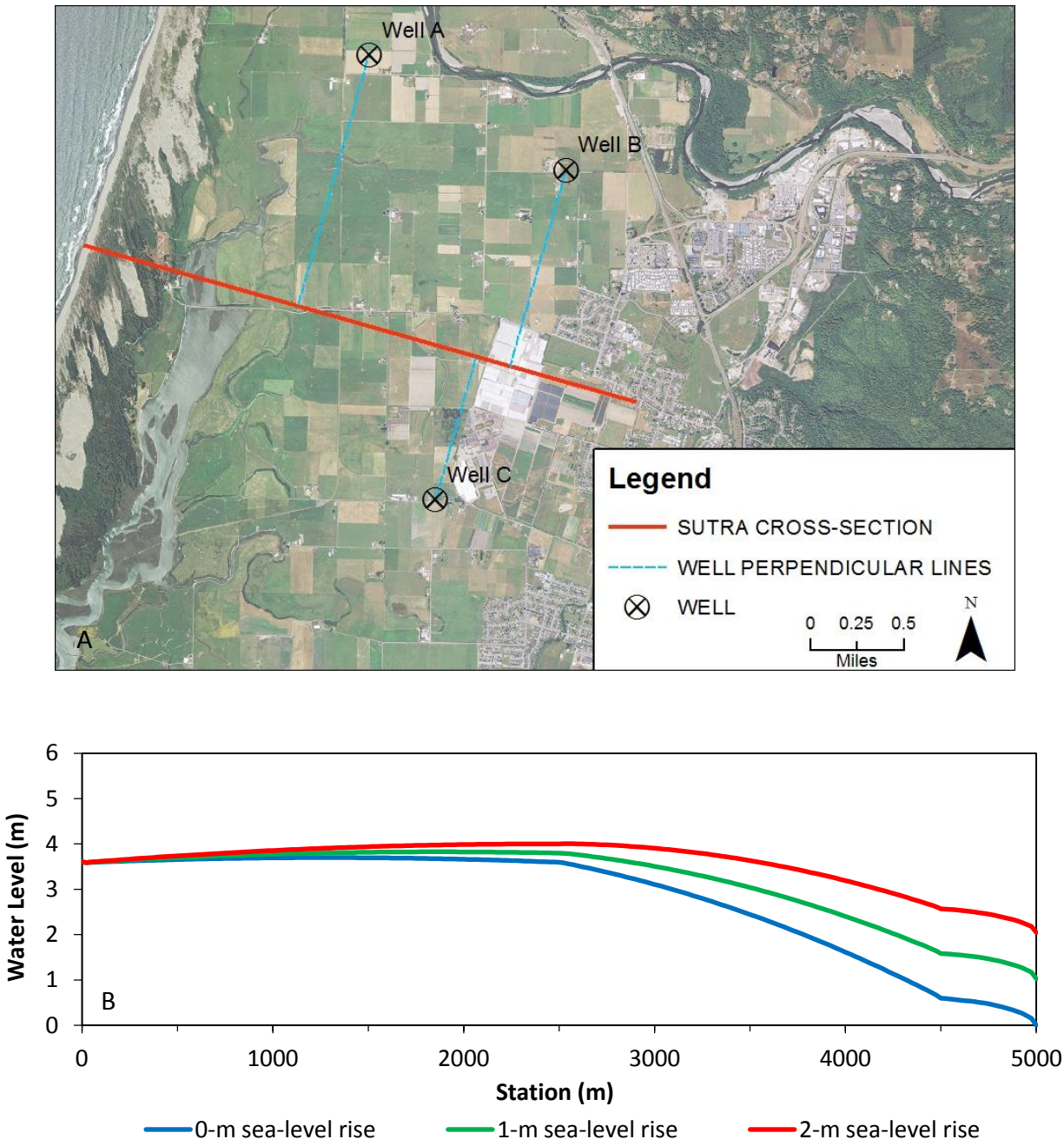

Figure 17. Location of conceptual groundwater model cross-section in Eureka-Arcata Plain and location of three Department of Water Resources wells (A), and groundwater level (hydraulic head) response of 0-, 1- and 2-meters of sea-level rise (B). Figures from Willis (2014).

coastal sites. Using a groundwater surface generated from groundwater elevation data obtained from three wells and topographic data developed using high-resolution digital elevation models (DEMs), Hoover et al. (2017) assessed the vulnerability of the Arcata region to sea-level rise driven groundwater emergence and shoaling with future sea-level rise scenarios of 1 and 2

meters (Figure 18). The analysis predicted 27% and 73% of the study area to be inundated from emergent groundwater with 1 and 2 meters of sea-level rise, respectively, compared with a 2.7% areal inundation for 2011 existing conditions. Due to the simplicity of the modeling approach, and since the effects of groundwater extraction and tidal forcing were neglected, these results were thought to be conservative, but informative, estimates of the actual areal extents of sea-level driven groundwater inundation (Hoover et al., 2017).

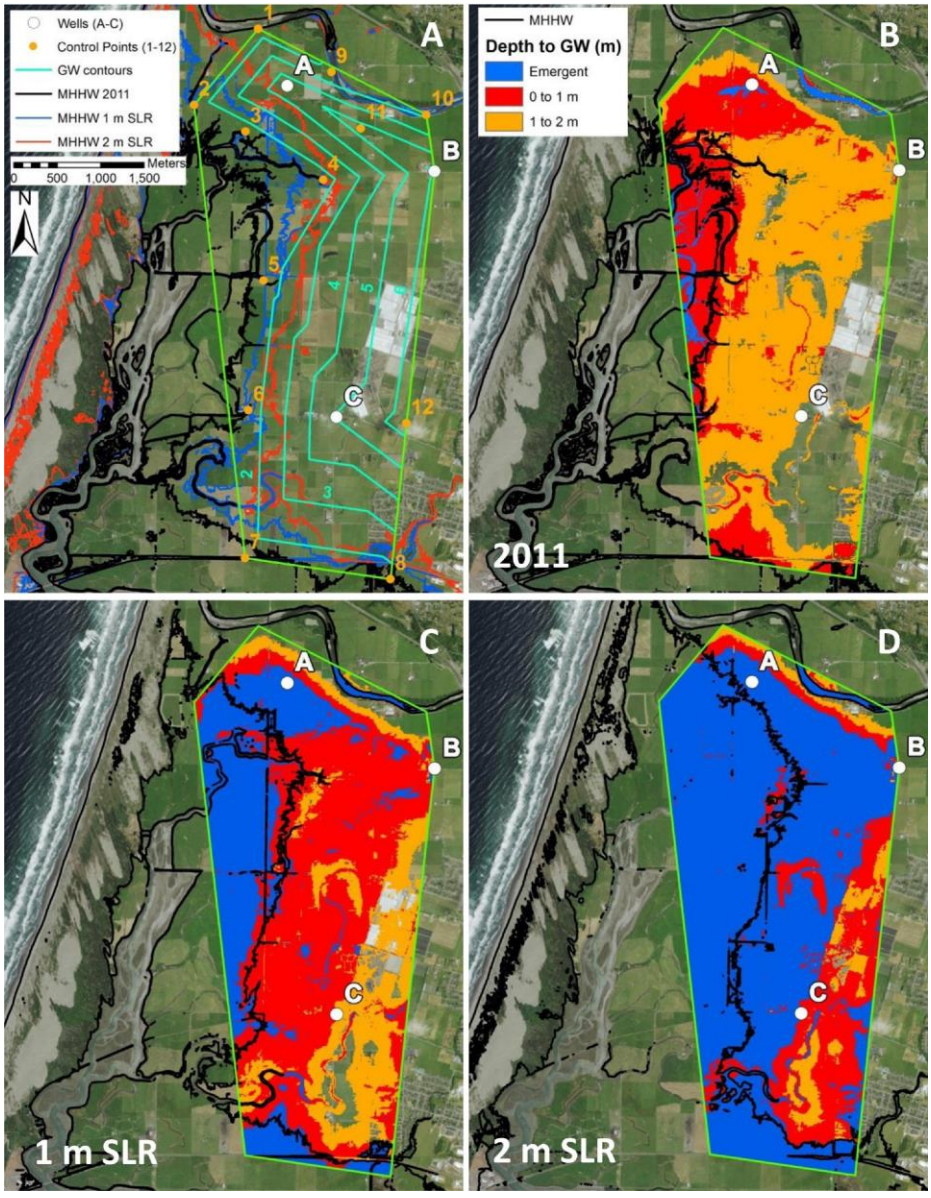

Figure 18. Sea-level rise driven groundwater emergence/shoaling in Arcata study area. Overview map showing well and boundary control point locations, resulting groundwater contours, and extent of inundation by present day MHHW, and 1 and 2 m increases (A). Calculated depths to groundwater for present-day conditions (B). Depth to groundwater for 1-m sea-level rise (C). Depth to groundwater for 2-m sea-level rise (D). Figure from Hoover et al. (2017).

As sea-level rise continues into the future, increases in groundwater levels within unconfined coastal aquifers can be expected, with potential adverse impacts to low-lying communities (Walter et al., 2016; Hoover et al., 2017). The degree of sea-level rise related groundwater inundation may vary substantially between different regions along the California coast. Since a significant amount of land near Arcata, CA is situated at elevations below 3 m (NAVD88), and typical MHHW levels range between 1.6 m and 2.0 m (NAVD88) throughout the California coast, Arcata was identified as "potentially vulnerable to sea-level rise driven groundwater emergence and shoaling" (Hoover et al., 2015).

Following is a brief list of potential impacts to low-lying areas of Arcata due to increased groundwater levels and inundation from sea-level rise:

- Rising groundwater levels can inundate and flood low-lying areas within Arcata, even if those areas are protected from surface water inundation by levees.
- Increased groundwater levels could impact current agricultural land and practices, and change/alter existing vegetation communities.
- Rising groundwater levels can alter surface water drainage patterns, impact existing stormwater drainage infrastructure, and limit the ability of low-lying areas to drain.
- Rainfall runoff and infiltrative characteristics of existing areas will change as groundwater levels increase. For example, unpaved areas that currently produce limited runoff due to infiltration of rainfall could generate more runoff as groundwater levels rise and infiltration capacity lessons. This type of rainfall/runoff response would create more runoff than currently exists from these low-lying areas, further impacting downstream stormwater infrastructure.
- Existing stormwater mitigation measures, such as detention and infiltration basins, swales, pervious pavements, etc., would become less effective as groundwater rises and infiltration capacity is reduced.
- Rising groundwater levels can increase Infiltration & Inflow into existing wastewater collection systems due to increased hydraulic head.
- Increased groundwater levels could impact existing residential and commercial onsite wastewater treatment and disposal systems in rural low-lying areas.

Glossary

AIS	Antarctic Ice Sheet
AR5	IPCC Fifth Assessment Report
CG	Cascadia Geosciences
CSZ	Cascadia subduction zone
ENSO	El Niño Southern Oscillation
GIA	glacial isostatic adjustment
GIC	glaciers and ice caps
GIS	Greenland Ice Sheet
GMSL	global mean sea level
GPS	global positioning system
IPCC	Intergovernmental Panel on Climate Change
LSL	local sea-level
LWS	land water storage
MAMW	mean annual maximum water
MEI	multivariate ENSO index
MHHW	mean higher high water
MMMW	mean monthly maximum water
MSL	mean sea level
NAVD88	North American Vertical Datum of 1988
NHE	Northern Hydrology and Engineering
NOAA	National Ocean and Atmospheric Administration
OPC	Ocean Protection Council
PDO	Pacific Decadal Oscillation
PNW	U.S. Pacific Northwest
RCP	representative concertation pathway
ReSL	regional sea-level
TE	thermal expansion
VLM	vertical land motion

References

Beckley, B.D, N.P. Zelensky, S.A. Holmes, F.G. Lemoine, R.D. Ray, G.T. Mitchum, S.D. Desai, and S.T. Brown. 2010. Assessment of the Jason-2 Extension to the TOPEX/Poseidon, Jason-1 Sea-Surface Height Time Series for Global Mean Sea Level Monitoring. *Marine Geodesy*, Vol 33, Suppl 1.

Bjerklie, D., J. Mullaney, J. Stone, B. Skinner, and M. Ramlow. 2012. Preliminary investigation of the effects of sea-level rise on groundwater levels in New Haven, Connecticut. U.S. Geological Survey Open-File Report 2012-1025.

Bromirski, P. D., A. J. Miller, R. E. Flick, and G. Auad. 2011. Dynamical suppression of sea level rise along the Pacific coast of North America: Indications for imminent acceleration. *J. Geophys. Res.*, 116, C07005.

Burgette, R. J., R. J. Weldon II, and D. A. Schmidt. 2009. Interseismic uplift rates for western Oregon and along-strike variation in locking on the Cascadia subduction zone. *J. Geophys. Res.*, 114, B01408.

Cayan D. R., P. D. Bromirski, K. Hayhoe, M. Tyree, M. D. Dettinger, and R. E. Flick. 2008. Climate change projections of sea level extremes along the California coast. *Climatic Change*, 87, 57–73.

Church, J. A. and N.J. White. 2006. A 20th century acceleration in global sea level rise, *Geophysical Research Letters*, 33, L01602.

Church, J. A., and N. J. White. 2011. Sea-level rise from the late 19th to the early 21st century. *Surv. Geophys.*, 32, 585–602.

Church, J.A., P.U. Clark, A. Cazenave, J.M. Gregory, S. Jevrejeva, A. Levermann, M.A. Merrifield, G.A. Milne, R.S. Nerem, P.D. Nunn, A.J. Payne, W.T. Pfeffer, D. Stammer and A.S. Unnikrishnan. 2013. Sea Level Change. In: Climate Change 2013: The Physical Science Basis. Contribution of Working Group I to the Fifth Assessment Report of the Intergovernmental Panel on Climate Change [Stocker, T.F., D. Qin, G.-K. Plattner, M. Tignor, S.K. Allen, J. Boschung, A. Nauels, Y. Xia, V. Bex and P.M. Midgley (eds.)]. Cambridge University Press, Cambridge, United Kingdom and New York, NY, USA.

Ghilani, C. D. 2010. *Adjustment Computations Spatial Data Analysis, Fifth Edition*. John Wiley & Sons, Inc. New Jersey.

Griggs, G, J. Árvai, D. Cayan, R. DeConto, J. Fox, H.A. Fricker, R.E. Kopp, C. Tebaldi, and E.A. Whiteman. 2017. Rising Seas in California: An Update on Sea-Level Rise Science. California Ocean Science Trust.

Grinsted, A., S. Jevrejeva, R.E.M Riccardo, and D. Dahl-Jensen. 2015. Sea level rise projections for northern Europe under RCP8.5. *Clim. Res.*, 64:15-23.

Habel, S. 2016. Modeling Sea Level Rise Induced Groundwater Inundation in Waikiki, Kaka'ako and Mo'ili'ili, O'ahu. University of Hawai'i at Manoa, Department of Geology and Geophysics, Honolulu, HI.

Hall, J.A., S. Gill, J. Obeysekera, W. Sweet, K. Knuuti, and J. Marburger. 2016. Regional Sea Level Scenarios for Coastal Risk Management: Managing the Uncertainty of Future Sea Level Change and Extreme Water Levels for Department of Defense Coastal Sites Worldwide. U.S. Department of Defense, Strategic Environmental Research and Development Program. 224 pp.

Hamlington, B.D., S.H. Cheon, P.R. Thompson, M.A. Merrifield, R.S. Nerem, R.R. Leben, and K.Y. Kim. 2016. An ongoing shift in Pacific Ocean sea level. *Journal of Geophysical Research: Ocean*s, 121(7), 5084-5097.

Hay, C.C., E. Morrow, R.E. Kopp, and J.X. Mitrovica. 2015. Probabilistic reanalysis of twentieth-century sea-level rise. *Nature*, 517(7535), 481-484.

Hoover, D., K. Odigie, P. Swarzenski, and P. Barnard. 2017. Sea-level rise and coastal groundwater inundation and shoaling at select sites in California, USA. *Journal of Hydrology: Regional Studies*, 11, 234-249.

IPCC. 2013. Summary for Policymakers. In: Climate Change 2013: The Physical Science Basis. Contribution of Working Group I to the Fifth Assessment Report of the Intergovernmental Panel on Climate Change [Stocker, T.F., D. Qin, G.-K. Plattner, M. Tignor, S.K. Allen, J. Boschung, A. Nauels, Y. Xia, V. Bex and P.M. Midgley (eds.)]. Cambridge University Press, Cambridge, United Kingdom and New York, NY, USA.

Knowles, N. 2010. Potential inundation due to rising sea levels in the San Francisco bay region. *San Francisco Estuary and Watershed Science*, 8(1).

Komar, P. D., J.C. Allan, and P. Ruggiero. 2011. Sea level variations along the U.S. Pacific Northwest Coast: tectonic and climate controls. *Journal of Coastal Research*: Volume 27, Issue 5: pp. 808 – 823.

Kominz, M. 2001. Sea Level Variations Over Geologic Time. In Encyclopedia of Ocean Sciences. Elsevier, 2605-2613.

Kopp, R.E., R.M. Horton, C.M. Little, J.X. Mitrovica, M. Oppenheimer, D.J. Rasmussen, B.H. Strauss, and C. Tebaldi. 2014. Probabilistic 21st and 22nd Century Sea-Level Projections at a Global Network of Tide-Gauge Sites. *Earth's Future*, 2:1–24.

Kopp, R.E., B.P. Horton, A.C. Kemp, and C. Tebaldi. 2015. Past and Future Sea-Level Rise along the Coast of North Carolina, USA. *Climatic Change*, 132:693–707.

Laird, A. 2013. Humboldt Bay Shoreline Inventory, Mapping and Sea Level Rise Vulnerability Assessment. Prepared for State Coastal Conservancy. Trinity Associates, Arcata, CA.

Mantua, N. J., S. R. Hare, Y. Zhang, J. M. Wallace, and R.C. Francis. 1997. A Pacific interdecadal climate oscillation with impacts on salmon production. *Bulletin of the American Meteorological Society*, 78, 1069-1079.

Maréchal, J. n.d. Establishment of earth tides effect on water level fluctuations in an unconfined hard rock aquifer using spectral analysis. Retrieved August 2017, from https://arxiv.org/ftp/arxiv/papers/1002/1002.3916.pdf.

Mitchell, C. E., P. Vincent, R. J. Weldon, and M. A. Richards. 1994. Present-day vertical deformation of the Cascadia margin, Pacific northwest, United States: *J. Geophys. Res*. 99(B6), 12,257-12,277.

Monachesi, L., and L. Guarracino. 2011. Exact and approximate analytical solutions of groundwater response to tidal fluctuations in a theoretical inhomogeneous coastal confined aquifer. *Hydrogeology Journal*, 19, 1443-1449.

National Research Council (NRC). 2012. Sea-Level Rise for the Coasts of California, Oregon, and Washington: Past, Present, and Future. The National Academies Press, Washington, DC.

Northern Hydrology & Engineering (NHE). 2015a. Humboldt Bay: Sea Level Rise, Hydrodynamic Modeling, and Inundation Vulnerability Mapping. Prepared for the State Coastal Conservancy, and Coastal Ecosystems Institute of Northern California. McKinleyville, CA.

Northern Hydrology & Engineering (NHE). 2015b. Technical Memorandum: Humboldt Bay Sea Level Rise Water Level Elevation Extraction Excel Application for Support of the City of Arcata Wastewater Treatment Facility Reconfiguration. Prepared for City of Arcata. McKinleyville, CA.

Patton, J. R., T. B. Williams, J. K. Anderson, and T. Leroy. 2017. Tectonic land level changes and their contribution to sea-level rise, Humboldt Bay region, Northern California: 2017 Final Report. Prepared for U.S. Fish and Wildlife Service Coastal Program. Cascadia GeoSciences, McKinleyville, CA.

Rhein, M., S.R. Rintoul, S. Aoki, E. Campos, D. Chambers, R.A. Feely, S. Gulev, G.C. Johnson, S.A. Josey, A. Kostianoy, C. Mauritzen, D. Roemmich, L.D. Talley and F. Wang. 2013. Observations: Ocean. In: Climate Change 2013: The Physical Science Basis. Contribution of Working Group I to the Fifth Assessment Report of the Intergovernmental Panel on Climate Change [Stocker, T.F., D. Qin, G.-K. Plattner, M. Tignor, S.K. Allen, J. Boschung, A. Nauels, Y. Xia, V. Bex and P.M. Midgley (eds.)]. Cambridge University Press, Cambridge, United Kingdom and New York, NY, USA.

Rotzoll, K. and A. El-Kadi. 2008. Estimating hydraulic properties of coastal aquifers using wave setup. *Journal of Hydrology*, 353(1-1), 201-213.

Rotzoll, K. and C. Fletcher. 2012. Assessment of groundwater inundation as a consequence of sea-level rise. *Nature Climate Change*, 3, 477-481.

Russell, N.and G. Griggs. 2012. Adapting to Sea Level Rise: A Guide to California's Coastal Communities. Prepared for the California Energy Commission Public Interest Environmental Research Program. University of California, Santa Cruz.

Sweet, W.V., R.E. Kopp, C.P. Weaver, J. Obeysekera, R.M. Horton, E.R. Thieler, and C. Zervas. 2017. Global and Regional Sea Level Rise Scenarios for the United States. NOAA Technical Report NOS CO-OPS 083. NOAA/NOS Center for Operational Oceanographic Products and Services.

Turner, I., B. Coates, and R. Acworth. 1997. Tides, Waves and the Super-elevation of Groundwater at the Coast. *Journal of Coastal Research*, 13(1), 46-60.

Walter, D., T. McCobb, J. Masterson, and M. Fienen. 2016. Potential effects of sea-level rise on the depth to saturated sediments of the Sagamore and Monomoy flow lenses on Cape Cod, Massachusetts (ver. 1.1, October 12, 2016). U.S. Geological Survey Scientific Investigations Report 2016-5058.

Willis, R. 2014. Conceptual Groundwater Model of Sea Level Rise in the Humboldt Bay Eureka-Arcata Coastal Plain. Prepared for State Coastal Conservancy, and Coastal Ecosystems Institute of Northern California. Arcata, CA.

Wolter, K., and M. S. Timlin. 1993. Monitoring ENSO in COADS with a seasonally adjusted principal component index. Proceedings of the 17th Climate Diagnostics Workshop, Norman, OK, NOAA/NMC/CAC, NSSL, Oklahoma Climate Survey, CIMMS and the School of Meteorology, University of Oklahoma: Norman, OK; 52–57.

Wolter, K., and M. S. Timlin. 1998. Measuring the strength of ENSO events – how does 1997/98 rank? *Weather* ,53, 315–324.

Wolter, K., and M. S. Timlin. 2011. El Niño/Southern Oscillation behaviour since 1871 as diagnosed in an extended multivariate ENSO index (MEI.ext). *Intl. J. Climatology*, 31(7), 1074-1087.

Zervas, C., S. 2009. Sea Level Variations of the United States 1854-2006. NOAA National Ocean Service Center for Operational Oceanographic Products and Services. NOAA Technical Report NOS CO-OPS 053. 78pp.

Zhang Y., J.M. Wallace, and D.S. Battisti. 1997. ENSO-like interdecadal variability: 1900–93. *J Clim* 10:1004–1020.